

Part I

Electron Diffraction Investigations of the Structures  
of Some Fifth Group Halides and of Quinone

Part II

Precipitation Reactions Between Antibodies  
and Benzoic Acid Derivatives

Part III

The Construction and Operation of a Tiselius  
Electrophoresis Apparatus

Thesis

by

Stanley M. Swingle

In Partial Fulfillment of the Requirements for the  
Degree of Doctor of Philosophy

California Institute of Technology

Pasadena, California

1943

## Table of Contents

<b>Part I. Electron Diffraction Investigations</b>	<b>1</b>
A. General Description of Methods Currently Employed	1
B. The Structures of the Trichlorides, Tribromides and Triiodides of Phosphorus, Arsenic and Antimony	4
a. Experimental	6
b. Discussion	26
c. Summary of results	27
C. A Discrepancy Between Long and Short Camera Pictures	30
D. The Structure of Quinone	34
a. Experimental	35
b. Results	43
c. Discussion	44
E. References	
<b>Part II. Precipitation Reactions Between Antibodies and     Benzoic Acid Derivatives</b>	<b>46</b>
A. Qualitative	46
a. Experimental	47
b. Results	53
c. Discussion	54
B. Quantitative	55
a. The effect of diluting agents	55
b. The effect of pH	56
c. The effect of simple haptens	60
d. Discussion	68
C. References	73
<b>Part III. A Tiselius Electrophoresis Apparatus</b>	<b>74</b>
A. Construction of the Apparatus	74
B. The Optimum Temperature for Electrophoresis	83
C. References	89
Summary	90
Acknowledgement	91
Propositions	92

Part I

Electron Diffraction Investigations of the Structures  
of Some Fifth Group Halides and of Quinone

Electron Diffraction Investigations of the Structures  
of some Fifth Group Halides and of Quinone

Electron diffraction is now a generally accepted tool of research, having distinct advantages over other methods of determining the structure of gaseous molecules. Applications of the technic to investigations of the structures of ten molecules of interest are presented in part I of this thesis.

General description of the methods currently employed.-- Diffraction photographs are prepared and analyzed with the apparatus and technic described by Brockway (1). Briefly, electrons from a hot tungsten filament are accelerated through a closely regulated electric field of about 40,000 volts. A pair of pin holes in thin brass spaced several centimeters apart defines a narrow beam of the electrons. This beam meets a fine jet of the substance being studied as it issues from a small orifice just below the beam. The electrons are scattered in a pattern characteristic of the substance. Several centimeters beyond the jet the electrons strike a photographic film which records their distribution. Exposures of about 1/5 to 2 seconds are usually sufficient.

The diffraction photographs appear to show a series of concentric diffuse rings decreasing in intensity from the center outward. The determination of the structure is based on a theoretical treatment (2,3,4,5,6) relating the distribution of scattering as observed on the photographs with the structure of the substance causing the scattering. According to the theory the intensity of scattered electrons is given by the equation

$$I \propto \frac{1}{s^5} \sum_i \sum_j' (Z_i - f_i)(Z_j - f_j) \frac{\sin sr_{ij}}{r_{ij}} + \text{background scattering} \quad (1)$$

The summations are over all the atoms in the molecule.

$Z_i$  = atomic number of atom i.

$f_i$  = atomic scattering factor for x-rays. This can often be omitted (7).

$$s = \frac{4\pi}{\lambda} \sin \frac{\phi}{2}$$

$\phi$  = the angle of scattering.

$\lambda$  = wavelength of electrons.

$r_{ij}$  = interatomic distance.

The background scattering (eq. 1) decreases monotonically from the center of the photographs outward and is of no value in determining the structure. The rest of the scattering function is seen to oscillate above and below the background giving rings decreasing progressively in intensity from the center outward. This is the part of the scattering that must be studied on the photographs.

It is the common practice here to determine the distribution of intensity on the photographs by visual inspection (7). One can observe the fluctuation in intensity above and below the general background and thus pick out the part of the scattering that is to be compared with equation (1). Indeed, the eye naturally tends to observe variations in density rather than the absolute value. Furthermore one can ignore the progressive decrease in intensity of the rings from the center outward and thus draw a curve (e.g. fig. 7 to 10) representing the appearance of the photographs exclusive of background and damping. This curve is to be compared with graphs of the theoretical intensity function (eq. 1) in the modified form

$$I \propto \sum_i \sum_j \frac{(z_i - f_i)(z_j - f_j)}{r_{ij}} \sin s r_{ij} \quad (2)$$

In the correlation method of determining the structure, a series of these theoretical intensity functions are evaluated for various models of the structure in question. The graphs of the intensity as a function of  $s$  (e.g. fig. 2 to 6) for these models are compared qualitatively with the photographs to determine which model gives the best agreement.

It should be noted that  $s = \frac{4\pi}{\lambda} \sin \frac{\phi}{2}$  is approximately proportional to the ring diameter so that a direct comparison is possible.

A quantitative comparison of the photographs with the theoretical intensity curves is made by determining the ratio of  $s$  for features on the theoretical intensity curves to  $s_0$  for the corresponding feature on the photographs. To obtain  $s_0$ , the diameters of the rings at maxima and minima are measured with a comparator. In measuring a particular feature, for example a maximum, the pointers of the comparator must be set at the point where the density differs most from the steeply sloping background rather than the point of greatest apparent density. A large number of measurements of each feature should be made to reduce random errors in setting the pointers. It is best to make only a few consecutive measurements at a time on one photograph to eliminate the natural tendency to memorize subconsciously the positions of particular features.  $\lambda$  is determined by calibration with transmission pictures of gold foil as often as is deemed necessary. The weighted average of  $s/s_0$  for the best model is a constant which multiplies all the interatomic distances assumed for this model to give the values in agreement with the photographs.

An alternative or supplement to the correlation method is based on the radial distribution equation (ref. 8) derived from equation (1). In the form as modified by Dr. Schomaker (9) this equation is

$$D(r) = \sum_k I_k s_k e^{-as_k^2} \frac{\sin s_k r}{s_k r} \quad (3)$$

where  $I_k$  is the estimated reduced intensity of the given feature and  $a$  in the artificial temperature factor has such a value that  $as^2$  is 1/10 for the last observable ring. The peaks of a plot of this function give the interatomic distance in the molecule directly.

An Investigation of the Structures of the Trichlorides,  
Tribromides, and Triiodides of Phosphorus,  
Arsenic, and Antimony

The determination of the structures of a series of closely related compounds is a valuable procedure for testing or deriving empirical generalizations regarding molecular structures, such as the additivity rule for covalent radii (10, 11, 12) and for formulating reasonable interpretations of observed deviations. An important and extensive series of this sort is formed by the trihalides of the fifth-group elements. Most of these compounds are well adapted to investigation by electron diffraction; they are readily volatilized in a high temperature nozzle, give good scattering, and involve the simplest of calculations since there are only two parameters to be evaluated. For the most part both interatomic distances contribute to the scattering to a sufficient degree for their reasonably accurate evaluation. It seemed worthwhile to carry out a careful investigation of the molecules of this series because in many cases the values previously reported by the several investigators (13, 14, 15) are much less consistent than might be expected. In this paper our results for the trichlorides, tribromides, and triiodides of phosphorus, arsenic, and antimony are presented and compared with those of previous workers. Work on the trifluorides is now in progress in These Laboratories.

Brockway and Wall (13) in 1934 first noted that the bond lengths in many non-metallic halides are appreciably less than the values predicted from the accepted covalent radii. They suggested the polar character of the bonds and their possible partial double bond character as probable causes for this effect. Brockway and Jenkins (16), and later Springall and Brockway (17), found that the additivity rule was obeyed by the methyl derivatives of these and other non-metals, where partial double bond formation was presumed to be impossible. This result seemed to show that the ionic character of the halide bonds is not responsible for the anomalies, since the set of methyl derivatives also included some molecules in

which the bonds were expected to be appreciably ionic. The significance of bond lengths in other halogen and methyl compounds has also received considerable attention (18, 19, 20, 21).

Gregg and coworkers (14) extended the investigations to include the more closely related halides discussed here. They interpreted their results (Table X) as indicating that both hypotheses together are needed to account for the observed bond lengths, but their explanation fails to consider the fact that many of the deviations, including the greatest one observed, that for phosphorus tri-iodide, are positive rather than negative. A year later Hassel and Sandbo (15) reported the results of an electron diffraction investigation including essentially the same set of compounds and showing similar deviations. It is to be noted that the disagreement with Gregg's results is greater than the limits of error reported (see ref. 21 for a revision of the estimated errors) and of roughly the same magnitude as the deviations from additivity under discussion. Schomaker and Stevenson (12) emphasized that partially ionic bonds are generally shorter than predicted by the additivity rule, and showed that a simple correction,  $-0.09 (x_i - x_j)$ , leads to better agreement especially for molecules composed of the lighter elements.

In view of the lack of agreement among the results reported by previous investigators for these molecules it may be well to discuss the accuracy which can be expected for these structure determinations. Comparisons of the results of the visual method in electron diffraction with those of spectroscopic and crystal structure studies have shown that interatomic distance values accurate to within 1% can be found by the electron diffraction method in all favorable cases. Examples of this degree of consistency are provided by allene (22), methyl acetylene (23), hexamethyl benzene (24), nitrous oxide and hydrazoic acid (25), and carbon dioxide and several diatomic molecules (26). We believe we have exercised sufficient care in this work to achieve this accuracy.

A discrepancy between long and short camera pictures of antimony triiodide was discovered after this work was essentially completed. Until this discrepancy is satisfactorily explained there is reason to question whether these and many previous electron diffraction investigations are accurate to better than 2% or more. The discrepancy is discussed separately at the end of the paper.

a. Preparation of Materials.--Merck's reagent grade antimony trichloride, Baker's c.p. arsenic trichloride, and Eastman white label phosphorus trichloride and tribromide were used without additional purification except that the antimony trichloride was distilled under reduced pressure as it had evidently taken up moisture. The only impurities likely to be present in significant amounts are the corresponding metal oxide or acid, and hydrogen halide resulting from hydrolysis. Of these the oxide is too involatile to cause trouble while the hydrogen halide, even if present in large amounts, would produce only a continuous background that would not affect the characteristic features of the diffraction pattern.

Antimony triiodide was prepared by direct combination of the elements using an excess of antimony. The product was washed with carbon disulfide, but the antimony was not removed as it is too involatile to cause trouble. m.p. 168°.

Arsenic triiodide and antimony tribromide were prepared by direct combination of the elements and were recrystallized from carbon disulfide. m.p. 144.5° and 96° respectively.

The arsenic tribromide was available from a previous investigation.

Phosphorus triiodide was prepared by direct combination of exactly equivalent portions of iodine and white phosphorus dissolved separately in purified carbon disulfide which was subsequently evaporated. m.p. 60.5°. About half of the sample was evaporated off in the diffraction apparatus before taking pictures in order to remove impurities which caused a general blackening of the earlier pictures. Since phosphorus triiodide is reported to be unstable

with heat, we took some pictures at temperatures considerably higher than necessary, but could detect no evidence of a shift in the rings such as would be caused by free iodine.

b. Experimental Method.--The diffraction photographs were prepared with a camera distance (jet to film) of 10.85 cm. Additional pictures of antimony triiodide were taken at 20.19 cm. to bring out details of the inner rings. Our photographs appear to be of much better quality than those obtained by previous investigators. As may be seen in Tables I to IX they generally show about 1 1/2 times as many rings as were previously reported (twice as many in two cases). In general ten or more photographs were made for each substance at the short camera distance and the best four or five were selected for measurement. The values of  $s_0 = \frac{4\pi}{\lambda} \sin \frac{\phi}{2}$  given in the tables are averages of values obtained by two observers each of whom made ten measurements on each ring. The average deviation between the two sets of measurements is 0.014 cm., about 0.7% of the average ring diameter.

Gregg et al. did not include measurements on minima in their calculations, because they believed that the eye is less sensitive to the minima. We have found that measurements of the apparent minima and maxima of the diffraction pattern are equally reliable. Indeed there is a tendency (27), which varies from observer to observer and with the method of observation of the photographs (26), for the maxima and minima to give values of the interatomic distances which are respectively too high and too low by equal amounts. This may account for the fact that Gregg's results are consistently higher than ours.

As the first step in analyzing the data, radial distribution curves (fig. 1) were prepared using equation (3). The vertical bars on the figure represent the values and estimated limits of error of the interatomic distances finally reported in this paper. The results given by the radial distribution function are recorded in Tables I to IX.

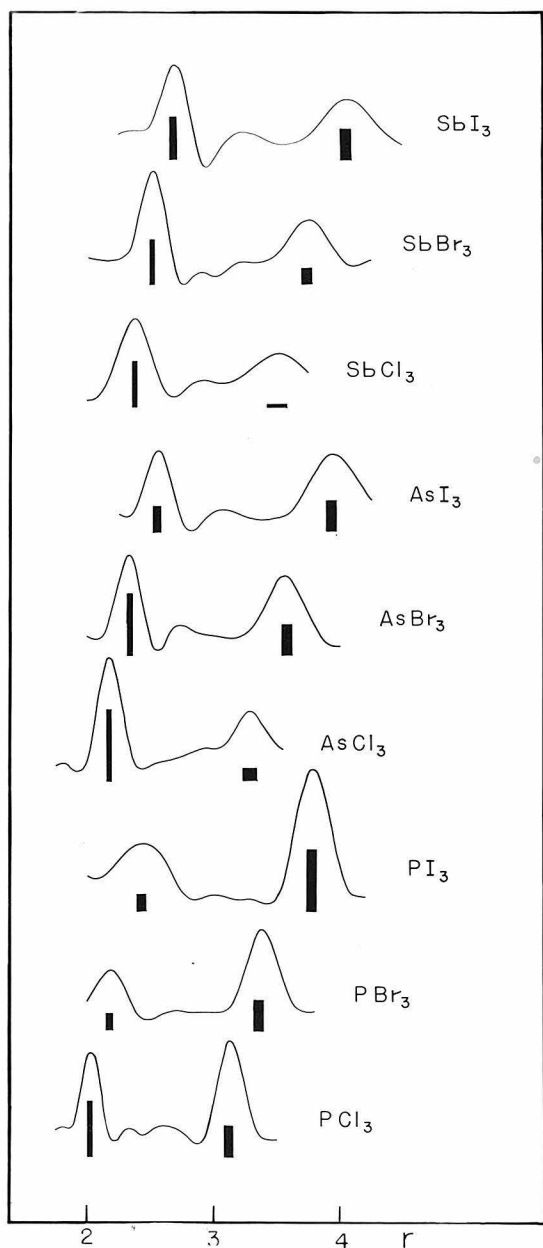


Figure 1  
Radial distribution curves with vertical bars representing the interatomic distances finally reported. The width of the bar represents the reported limits of error. The area gives the relative magnitude of the contribution to the scattering.

Further selection from among a few molecular models with the X-M-X angle varied by increments of  $2^\circ$  from that given by the radial distribution function was then made by the usual correlation method. The positions and general appearance of features on the photograph were compared with simplified theoretical intensity functions (eq. 2) in the form

$$I_{OC} = \frac{Z_M - f_M}{Z_X - f_X} \frac{\sin s r_{M-X}}{s r_{M-X}} + e^{-as^2} \frac{\sin s r_{X-X}}{s r_{X-X}} \quad (4)$$

(see fig. 2 to 6) using the  $r_{M-X}$  distance given by the radial distribution function. (For phosphorus triiodide the  $r_{X-X}$  distance was used.) The arrows on the curves were drawn at the positions where maxima and minima were measured on the photographs. For these molecules it is important to use the corrected relative scattering factors as in equation (4) rather than the simplified factors involving only the atomic numbers. Furthermore we found it necessary to apply a temperature factor to the X-X terms before a good fit was obtained. In some cases it was found possible to evaluate  $a = 1/2 \delta r_{X-X}^2 - 1/2 \delta r_{M-X}^2$  of the temperature factor as a third parameter (28).

Gregg et al. generally compared the fine structure of only a few of the most characteristic maxima with the various theoretical curves to eliminate models differing in the X-M-X bond angle by more than  $4^\circ$  from the one selected as correct. They based their selection of the most compatible theoretical curve largely on the positions of the maxima as expressed in the average deviations of  $s/s_0$ . We find that making a detailed comparison of the appearance of the photographs with the theoretical curves is a more sensitive method. The model chosen in this way generally shows the smallest average deviation in  $s/s_0$  as may be seen in the tables. However in the case of phosphorus triiodide and antimony triiodide slightly different results are obtained by the two methods of correlation.

This may result from omitting measurements on several features sensitive to variations in the model when taking the averages.

All of the photographs show much the same characteristic features because the molecules are all pyramidal with nearly the same bond angle, but the relative intensities of these features vary according to the relative magnitudes of the M-X and X-X scattering factors. The regions on the photographs most useful in determining the correct structures occur near the fourth, seventh, tenth, and thirteenth maxima of the X-X contribution to the scattering. In the cases where the corresponding characteristics were observed on the photographs, these regions are designated by the dashed lines labeled a, b, c, and d respectively in figures 2 to 6.

The first ring on all these photographs appears much more pronounced than is indicated by the theoretical curves. Even in the case of antimony trichloride it stands out clearly although the corresponding hump in the theoretical curves is almost imperceptible. Similar phenomena have been observed in many cases for rings near the central image where the background intensity is decreasing rapidly, especially if a weak ring or shelf is present. The steeply sloping background also adds uncertainty to observations in the vicinity of the fourth maximum from the X-X scattering (regions a on the theoretical curves). It is especially difficult to decide exactly on the relative depths of the minima on either side of this feature in those cases where this ring was visible, although these features were nevertheless valuable in determining the correct model. The corresponding maximum is not apparent for arsenic trichloride and antimony trichloride and tribromide but does affect the symmetry and depth of the fourth minimum in a manner sensitive to variations in the bond angle.

Useful features similar to those at a appear at b on all the photographs and are not greatly influenced by the background. By viewing superimposed pairs of photographs to increase the apparent contrast it is possible to correlate the regions marked c with the theoretical curves in all but three cases. This method also shows

characteristic features at d in the highly favorable cases of phosphorus trichloride and tribromide. The degree to which we feel sure of the correlation is indicated by the limits of error placed on the reported bond angles. The appropriate temperature factors were estimated from the appearance of the photographs in regions of large s.

Table I. Antimony Triiodide

Max.	Min.	$c_k^a$	$s_o^b$	$s_o^c$	$s_o^d$	Model I $s/s_o^b$	Model II $s/s_o^b$
	2		2.44				
2		4	3.36		3.28	(0.965)	(0.954)
	3	-7	4.17		4.32	1.000	.997
3		10	5.17	4.99	5.02	0.991	.981
	4	-1	5.96			(1.019)	(1.010)
4		3	6.58			(1.033)	(1.000)
	5	-4	7.11			(0.986)	(0.972)
5		11	7.85	7.70	7.80	(1.007)	(1.001)
	6	-11	8.77		8.90	1.010*	1.003*
6		11	9.85	9.63	9.54	0.996*	0.991*
	7	-11	10.97			(0.991)	(1.019)
7		10	12.33	12.29	11.94	(1.012)	(1.009)
	8	-9	13.33		13.42	1.014*	1.009*
8		9	14.52	14.13	14.37	1.000*	0.995*
	9	-8	15.58			1.010	1.024
9		7	16.84			1.014	1.011
	10	-5	17.93			1.014	1.010
10		5	19.11			1.007	1.007
	11	-4	20.12			1.011	1.021
11		3	21.34			1.017	1.014

From R. D. Sb-I = 2.68 Å., angle = 99°

Model	angle	"a"	$s/s_o^b$	ave. dev. in $s/s_o^b$
			ave.	
I	98°	0.004	1.007	0.0069
II	100°	.004	1.004	.0087
IIIA	100°	.002		
III	102°	.004	1.001	.0106
IIIA	102°	.002		
IV	104°	.004		

Final result: Sb-I = 2.67 Å.  $\pm$  0.03 Å.

angle = 99°  $\pm$  1°

"a"  $\approx$  0.003

a The coefficient,  $I_k s_k e^{-as_k}$ , of the radial distribution equation (3).

b This paper.

c Gregg et al.

d Hassel and Sandbo

Values not included in taking the average are in parentheses.

\* These values are given double weight.

These notations are used throughout the paper.

Table II  
Antimony Tribromide

Max.	Min.	$C_k^a$	$s_o^b$	$s_o^c$	$s_o^d$	Model IIA	Model IIIA
					$s/s_o^b$	$s/s_o^b$	
	1	-3	1.57				
1		1	3.18				
	2	-1	2.69				
2		6	3.61	3.41	4.66	(0.942)	(0.928)
	3	-8	4.56			.986	.980
3		9	5.52	5.51	5.51	1.000*	.996*
	4	-9	6.50			1.016	1.011
4		10	8.44	8.38	8.41	0.995	0.994
	5	-12	9.50			9.78	1.000*
5		13	10.53	10.62	10.66	1.002*	.996*
	6	-9	11.78			12.21	0.985
6		9	13.27	13.30	13.28	1.008	1.009
	7	-11	14.47			14.74	1.006*
7		10	15.55			15.68	1.002*
	8	-9	16.76				0.998
8		8	18.06				1.007
	9	-6	19.15				1.010
9		5	20.40				1.017
	10	-5	21.50				1.018
10		4	22.76				1.012

From R. D Sb-Br = 2.51 Å., angle = 97°

Model	angle	"a"	$s/s_o^b$ ave.	ave. deg. in $s/s_o^b$
I	94°	0.004		
II	96°	.004	1.000	0.0091
IIA	96°	.002	1.002	.0086
III	98°	.004	1.000	.0103
IIIA	98°	.002	1.000	.0099
IV	100°	.004		

Final result: Sb-Br = 2.51 Å.  $\pm$  0.02 Å.  
angle = 97°  $\pm$  2°  
"a"  $\approx$  0.003

Table III  
Antimony Trichloride

Max.	Min.	$c_k^a$	$s_o^b$	$s_o^c$	Model III $s/s_o^b$
	1	- 5	1.64		
1		7	2.36		
	2	- 2	2.86		
2		6	3.63	3.61	(0.943)
	3	-16	4.73		.996
3		18	5.86	5.84	1.007
	4	-13	7.13		1.003
4		16	8.71	8.65	0.993
	5	-19	10.03		.998
5		17	11.27	11.22	.996
	6	-15	12.44		1.005
6		13	13.82	13.88	1.006
	7	-10	15.22		1.005
7		8	16.56		1.001

From R. D. Sb-Cl = 2.37 Å., angle = 96°

Model	angle	"a"	$s/s_o^b$ ave.	ave. dev. in $s/s_o^b$
I	92°	0.004	1.002	0.0076
II	94°	.004	1.001	.0046
III	96°	.004	1.001	.0042
IV	98°	.004	1.000	.0054
V	100°	.004	0.999	.0074

Final result: Sb-Cl = 2.37 Å.  $\pm$  0.02 Å.  
angle = 96°  $\pm$  4°

Arsenic I. I. de

					Model	Model	
Max.	Min.	$c_k^a$	$s_0^b$	$s_0^c$	$s_0^d$	$s/s_0^b$	III
							$b$
1	1	- 3	1.39			(0.936)	(0.921)
1	2	- 2	2.04			(.995)	(.995)
2	2	- 3	2.67			.996	.974
2	5	- 5	3.55		3.65	.972	.958
3	3	- 8	4.34		4.52	.996	.991
3	4	- 4	5.27	5.24	5.30	1.000*	.993*
4	3	- 3	6.00			(1.033)	(1.021)
4	5	- 6	6.84	6.84	6.67	(0.995)	(0.970)
5	5	- 6	7.48		7.54	(.986)	(.971)
5	10	- 10	8.28	8.20	8.27	.998	.991
6	6	- 11	9.17		9.36	1.002*	.995*
6	10	- 10	10.22	9.97	10.14	0.994	.988
7	7	- 8	11.74		12.20		(1.017)
7	9	- 9	12.98	12.89	12.85	1.007	0.999
8	8	- 9	14.04			1.001*	.995*
8	7	- 7	15.22			0.994	.994
9	9	- 7	16.45			1.021	1.018
9	5	- 5	17.83			1.000	0.995
10	10	- 5	19.06			0.997	.992
10	3	- 3	20.28			.992	1.002

From R. D. As-I = 2.56 Å., angle = 100°

Model	angle	"a"	$s/s_0^b$	ave. dev.
			ave.	in $s/s_0^b$
I	98°	0.004		
II	100°	.004	1.000	0.0056
IIA	100°	.002	1.000	.0081
III	102°	.004	0.992	.0071
IIIA	102°	.002	.991	.0086
IV	104°	.004		

Final result: As-I = 2.55 Å.  $\pm$  0.03 Å.

angle = 101°  $\pm$  1.5°

"a"  $\approx$  0.004

Table V  
Arsenic Tribromide

						Model II
Max.	Min.	$c_k^a$	$s_o^b$	$s_o^c$	$s_o^d$	$s/s_o^b$
	1	- 3	1.54			
1		3	2.30			(1.028)
	2	- 2	3.01			(0.930)
2		6	3.89			(.944)
	3	- 8	4.84		5.00	.975
3	4	11	5.78	5.72	5.81	1.000*
	4	- 5	6.73			(1.033)
4		2	7.47	7.51	7.54	(1.002)
	5	- 6	8.21			(0.954)
5		11	9.08	8.96	9.10	.984*
	6	- 13	10.15		10.29	.992*
6		12	11.20	11.09	11.10	.996
	7	- 10	12.88		13.19	(1.004)
7		11	14.33	14.12	14.16	0.994*
	8	- 10	15.41		15.58	.999*
8		9	16.74		16.37	.991
	9	- 8	18.00			1.013*
9		7	19.50			1.000*
	10	- 6	20.60			1.008
10		5	22.14			0.999

From R. D. As-Br = 2.32 Å., angle = 100°

Model	angle	"a"	$s/s_o^b$ ave.	ave. dev. in $s/s_o^b$
I	98°	0.004		
II	100°	.004	0.996	0.0073
IIIA	100°	.002	.997	.0082
III	102°	.004	.993	.0088
IIIA	102°	.002	.993	.0103
IV	104°	.004		

Final result: As-Br = 2.33 Å.  $\pm$  0.02 Å.  
angle = 100.5°  $\pm$  1.5°  
"a"  $\approx$  0.004

Table VI  
Arsenic Trichloride

Max.	Min.	C <sup>a</sup> k	s <sup>b</sup> s <sub>0</sub>	s <sup>e</sup> s <sub>0</sub>	Model	Model
					III	IV
	1	-7	1.76			
1		5	2.52			
	2		3.05			
2		14	4.06	3.94	(0.960)	(0.953)
	3	-18	5.14	5.28	.996	.996
3		22	6.32	6.23	1.008	1.000
	4	-15	7.80	7.86	0.996	1.000
4		22	9.58	9.55	.999	0.996
	5	-28	10.83	11.00	1.002	1.001
5		28	12.10	12.13	1.009	1.005
	6	-22	13.62		1.007	1.019
6		23	15.35		0.995	0.997
	7	-24	16.61		1.002	1.002
7		22	17.94		1.007	1.007
	8	-15	19.35		1.009	1.011
8		13	20.98		1.001	1.003
	9	-12	22.44		1.001	1.001
9		9	24.10		0.993	0.993

From R. D. As-Cl = 2.17 Å., angle = 98°

Model	angle	"a"	s/s <sup>b</sup> ave.	ave. dev. in s/s <sup>b</sup> ave.
I	94°	0.004		
II	96°	.004	1.000	0.0079
III	98°	.004	1.000	.0048
IIIA	98°	.002	1.000	.0047
IIIB	98°	.000	1.000	.0055
IV	100°	.004	1.000	.0048
V	102°	.004	1.001	.0093

Final result: As-Cl = 2.17 Å.  $\pm$  0.02 Å.  
angle = 99°  $\pm$  2°  
"a"  $\approx$  0.003

e Brockway and Wall

Table VII  
Phosphorus Triiodide

Max.	Min.	$a_k^a$	$s_o^b$	$s_o^c$	$s_o^d$	Model III $s/s_o^b$
	1	- 5	1.35			(0.941)
1		6	2.07			(1.007)
	2	- 7	2.78		3.05	1.008
2		11	3.73	3.67	3.62	0.974
	3	-14	4.47		4.66	1.017
3		14	5.47	5.37	5.32	0.992
	4	-10	6.21		6.38	1.013
4		9	7.13	7.06	6.97	0.986
	5	-13	7.80		7.96	1.001
5		16	8.72	8.60	8.61	0.996
	6	-19	9.48		9.68	1.010
6		14	10.46	10.38	10.33	0.999
	7	- 9	11.18		11.60	1.009
7		8	12.15		12.27	0.988
	8	- 9	12.76			1.007
8		10	13.72			0.996
	9	- 7	14.48			1.010
9		7	15.46			0.998
	10	- 7	16.17			1.005
10		6	17.05			0.996

From R. D. I-I = 3.78 Å., angle = 102°

Model	angle	"a"	$s/s_o^b$ ave.	ave. dev. in $s/s_o^b$
I	98°	0.000		
II	100°	.000	1.000	0.0088
III	102°	.000	1.000	.0089
IV	104°	.000	1.000	.0079
V	106°	.000	0.998	.0088

Final result: P-I = 2.43 Å.  $\pm$  0.04 Å.

angle = 102°  $\pm$  2°

"a" < 0.000

Table VIII  
Phosphorus Tribromide

Max.	Min.	$C_k^a$	$s_o^b$	$s_o^c$	Model IIIA
	1	- 3	1.55		
1		4	2.40		(0.992)
	2	- 5	3.14		(.981)
2		7	4.15	4.04	.965
	3	- 8	5.07		1.000
3		10	6.13	6.00	0.999*
	4	- 5	6.97		1.017
4		4	7.91	7.76	0.991
	5	- 8	8.69		.998
5		11	9.74	9.55	.991*
	6	-11	10.60		1.010*
6		11	11.69	11.49	1.001
	7	- 3	12.45		1.014
7		3	13.44	13.30	0.994
	8	- 5	14.25		.998
8		8	15.23		.999*
	9	- 7	16.12		1.011
9		5	17.30		0.999
	10	- 1	18.04		1.007
10		2	18.94		0.991
	11	- 2	19.68		1.005
11		2	20.68		1.009

From R. D.  $P-Br = 2.18 \text{ \AA.}$ , angle =  $102^\circ$

Model	angle	"a"	$s_o^b$ ave.	ave. dev. in $s_o^b$
I	$98^\circ$	0.000		
II	$100^\circ$	.000	1.012	0.0077
III	$102^\circ$	.000	1.000	0.0074
IIIA	$102^\circ$	.001	1.000	0.0074
IIIB	$102^\circ$	.002	0.999	0.0092
IV	$104^\circ$	.000	0.987	0.0087

Final result:  $P-Br = 2.18 \text{ \AA.} \pm 0.03 \text{ \AA.}$   
angle =  $101.5^\circ \pm 1.5^\circ$   
"a" < 0.001

Table IX  
Phosphorus Trichloride

Max.	Min.	$C_k^a$	$s_o^b$	$s_o^e$	Model IIIA
					$s/s_o^b$
	1	-7	1.73		(0.983)
1		6	2.65	2.76	(1.019)
	2	-5	3.29	3.57	(0.976)
2		16	4.42	4.54	.965
	3	-19	5.45	5.63	1.001
3		23	6.60	6.66	1.002*
	4	-13	7.54	8.75	(1.041)
4		11	8.50	10.38	(0.994)
	5	-20	9.26	11.62	(.995)
5		30	10.37	12.58	.996*
	6	-30	11.46		1.008*
6		31	12.69		1.003
	7	-12	13.56		(1.019)
7		6	14.50		(0.994)
	8	-18	15.29		.991
8		29	16.41		.997*
	9	-27	17.53		1.002
9		20	18.94		0.996
	10	-17	20.95		1.014
10		19	22.40		1.001*
	11	-17	23.77		1.000
11		14	25.27		
	12	-12	16.84		1.017
12		9	28.49		0.999

From R. D.  $P-Cl = 2.03 \text{ \AA.}$ , angle =  $101^\circ$

Model	angle	"a"	$s/s_o^b$ ave.	ave. dev. in $s/s_o^b$
I	$97^\circ$	0.000		
II	$99^\circ$	0.000	1.009	0.0075
III	$101^\circ$	0.000	1.000	0.0071
IIIA	$101^\circ$	.001	1.000	.0059
IIIB	$101^\circ$	.002	1.000	.0081
IV	$103^\circ$	.000	0.995	.0074

Final result:  $P-Cl = 2.03 \text{ \AA.} \pm 0.02 \text{ \AA.}$   
 $\text{angle} = 100.5^\circ \pm 1.5^\circ$   
 $"a" \approx 0.001$

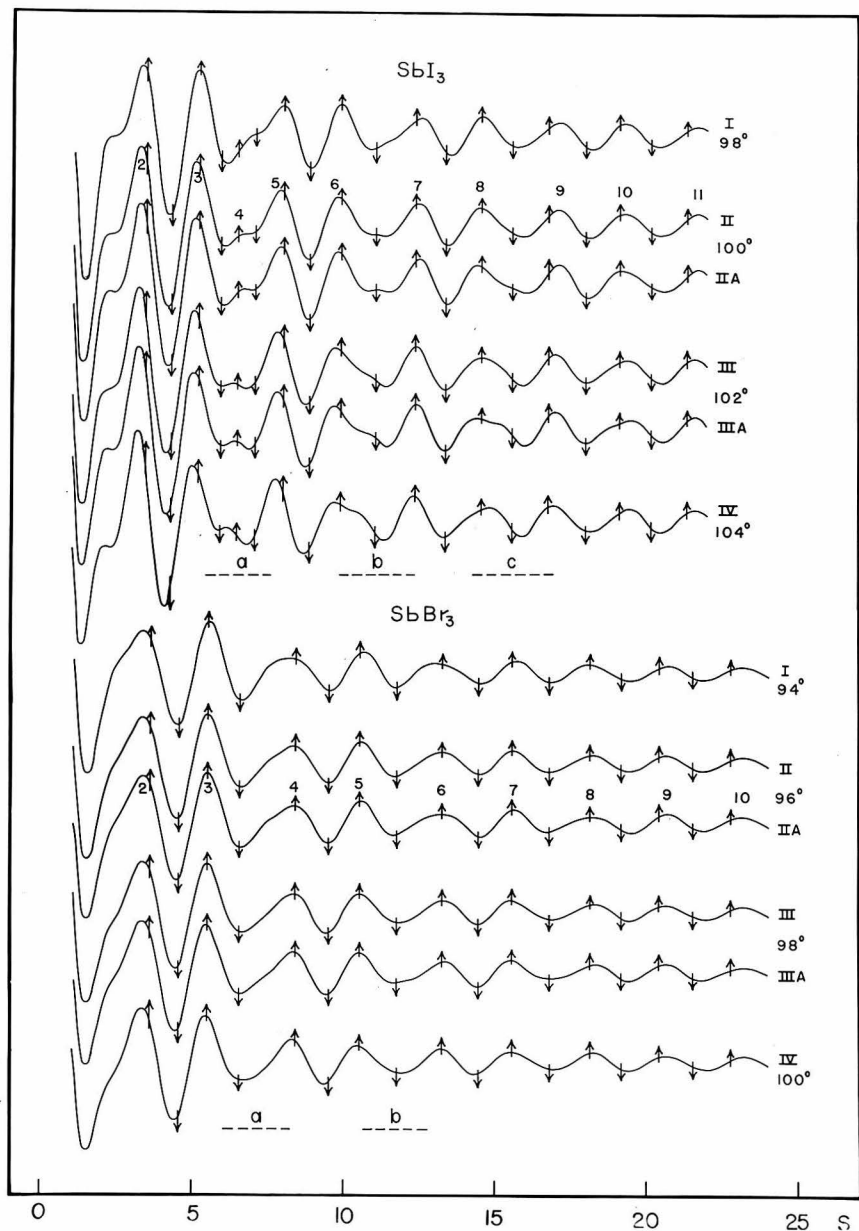


Figure 2  
Theoretical intensity curves  
a, b, c, regions especially useful in determining  
the structure.

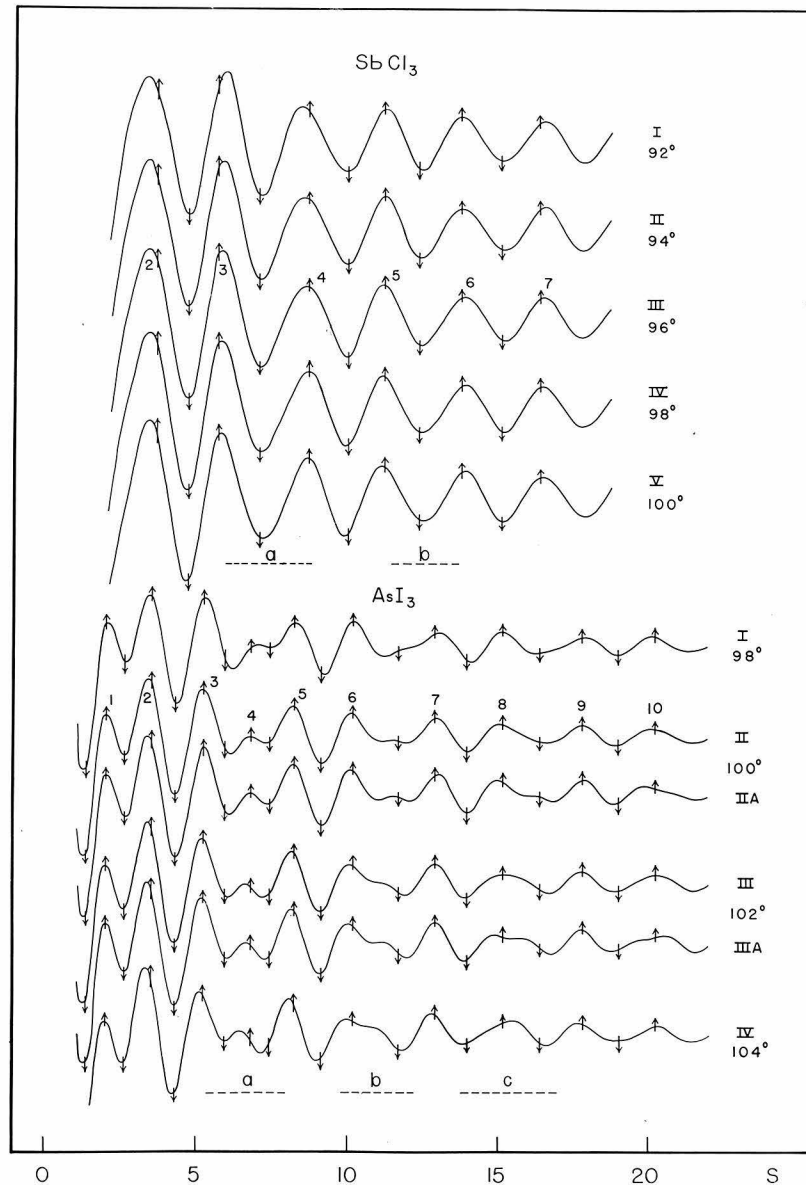


Figure 3  
Theoretical Intensity Curves

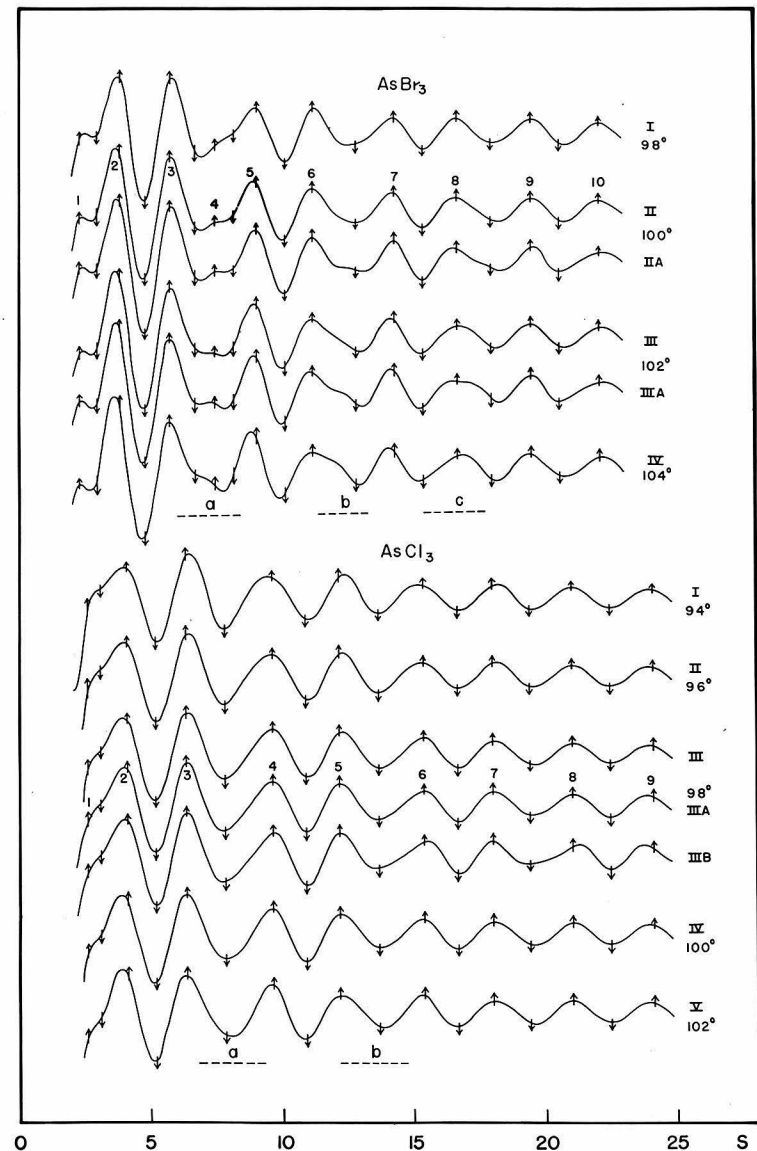


Figure 4  
Theoretical Intensity Curves

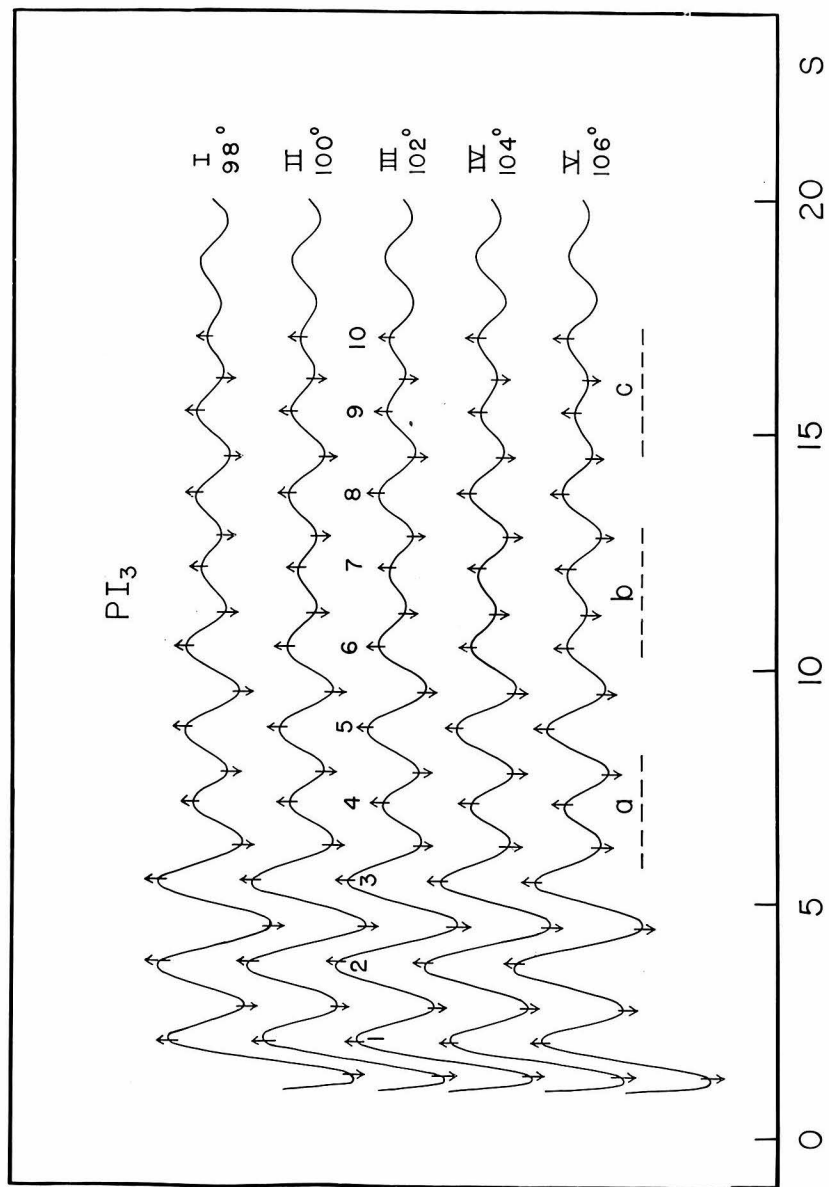


Figure 5  
Theoretical Intensity Curves

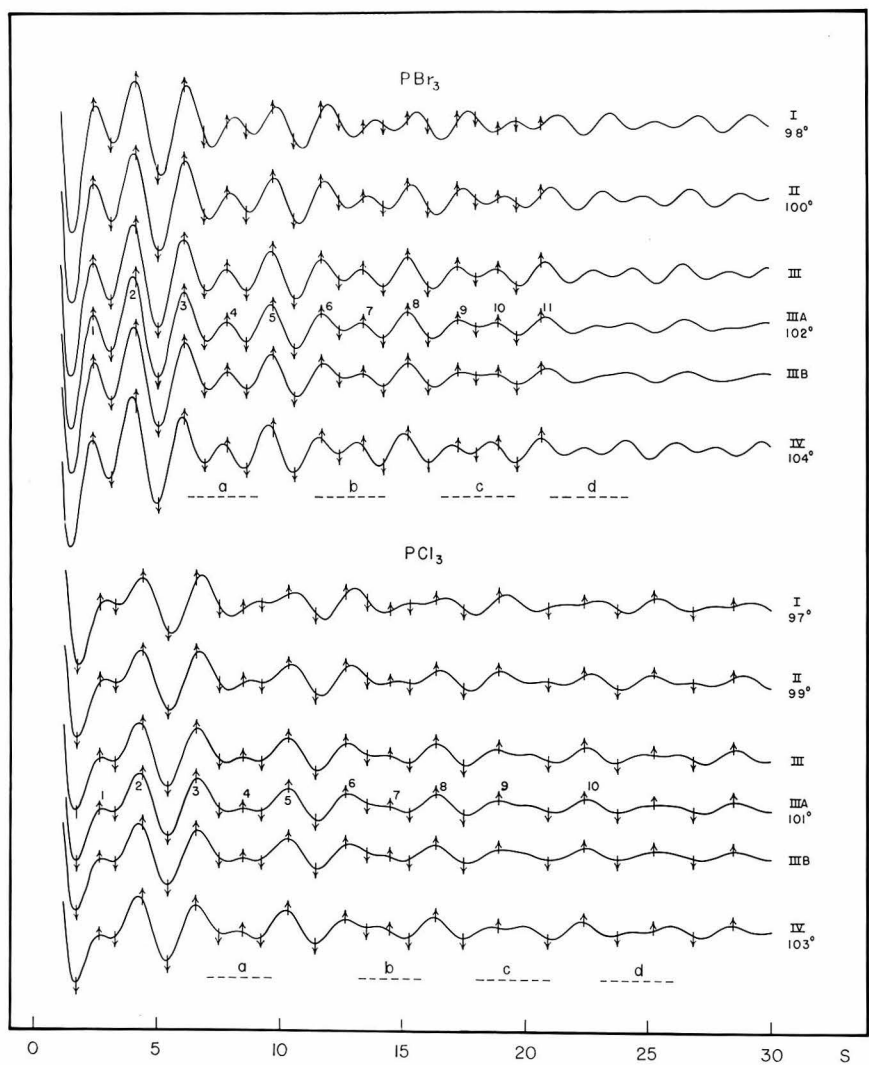


Figure 6  
Theoretical Intensity Curves

#### Discussion

The results of these investigations are tabulated beside those of previous investigators for convenience (Table X). Deviations from the Pauling-Huggins additivity rule and the modified rule of Schomaker and Stevenson are shown in Table XI. It seems confirmed beyond all reasonable doubt that these deviations are beyond the range of experimental error, but it seems fruitless to attempt an explanation at present due to the various uncertainties involved and the small magnitude of the discrepancies under discussion. It may be that the accepted atomic radii and electronegativities are not satisfactory as may be the case for arsenic and antimony.

The bond angles, recorded in Tables XII for convenience, form a very systematic set of values which may be significant. The X-X distances are less than the Van der Waal's diameters suggesting, as Lister and Sutton (21) have mentioned, that corresponding steric forces tending to widen the bond angle and possibly affect the bond length are present. The magnitudes of these differences, listed under the angles in Table XII, correlate well with the bond angles. The trends of the observed a values of the temperature factor given in Table XIII seem reasonable from our knowledge of the relative masses and expected force constants for these molecules and the temperatures at which the pictures were taken.

Table X  
Summary of Results

		M-X bond length Å.	angle	Obs.	non-bonded X-X sepn. Å.
SbI <sub>3</sub>	<sup>a</sup> 2.74	<sup>c</sup> 2.68 $\pm$ 0.03	99° $\pm$ 1°	4.06	<sup>g</sup> 4.30
	<sup>b</sup> 2.69	<sup>d</sup> 2.75 $\pm$ 0.05	98° $\pm$ 2°	4.16	
		<sup>e</sup> 2.70	99°	4.10	
SbBr <sub>3</sub>	2.55	<sup>c</sup> 2.51 $\pm$ 0.02	97° $\pm$ 2°	3.76	3.90
	2.46	<sup>d</sup> 2.52 $\pm$ 0.03	96° $\pm$ 2°	3.74	
		<sup>e</sup> 2.47	98°	3.72	
SbCl <sub>3</sub>	2.40	<sup>c</sup> 2.37 $\pm$ 0.02	96° $\pm$ 4°	3.52	3.60
	2.29	<sup>d</sup> 2.37 $\pm$ 0.02	104° $\pm$ 4°	3.74	
AsI <sub>3</sub>	2.54	<sup>c</sup> 2.55 $\pm$ 0.03	101° $\pm$ 1.5°	3.94	4.30
	2.50	<sup>d</sup> 2.58 $\pm$ 0.05	100° $\pm$ 2°	3.95	
		<sup>e</sup> 2.51	102.5°	3.92	
AsBr <sub>3</sub>	2.35	<sup>c</sup> 2.33 $\pm$ 0.02	100.5° $\pm$ 1.5°	3.59	3.90
	2.28	<sup>d</sup> 2.36 $\pm$ 0.04	100° $\pm$ 2°	3.62	
		<sup>e</sup> 2.31	101.5°	3.58	
AsCl <sub>3</sub>	2.20	<sup>c</sup> 2.17 $\pm$ 0.02	99° $\pm$ 2°	3.30	3.60
	2.11	<sup>f</sup> 2.18 $\pm$ 0.03	101° $\pm$ 4°	3.36	
PI <sub>3</sub>	2.43	<sup>c</sup> 2.43 $\pm$ 0.04	102° $\pm$ 2°	3.78	4.30
	2.40	<sup>d</sup> 2.52 $\pm$ 0.07	98° $\pm$ 4°	3.81	
		<sup>e</sup> 2.42 $\pm$ 0.04	102.5° $\pm$ 2.5°	3.78	
PBr <sub>3</sub>	2.24	<sup>c</sup> 2.18 $\pm$ 0.03	101.5° $\pm$ 1.5°	3.37	3.90
	2.18	<sup>d</sup> 2.23 $\pm$ 0.04	100° $\pm$ 2°	3.42	
PCl <sub>3</sub>	2.09	<sup>c</sup> 2.03 $\pm$ 0.02	100.5° $\pm$ 1.5°	3.13	3.60
	2.01	<sup>f</sup> 2.02 $\pm$ 0.02	101° $\pm$ 2°	3.12	

<sup>a</sup> Sum of covalent radii (11).

<sup>b</sup>  $r_M + r_X - 0.09(X-X)_M$  (12).

<sup>c</sup> This paper.

<sup>d</sup> Gregg et al. (14, 21)

<sup>e</sup> Hassel and Sandbo (15)

<sup>f</sup> Hassel and Sandbo (15)

<sup>g</sup> Brockway and Wall (13)

<sup>g</sup> Pauling's Van der Waals diameters (11) Table 24.1.

Table XI

Deviations from Additivity

	I	Br	Cl
Sb	-0.06 <sup>a</sup> - .01 <sup>b</sup>	-0.04 .05	-0.03 .08
As	.01 .05	- .02 .05	- .03 .06
P	.00 .03	- .06 .00	- .06 .02

a  $(r_{M-X})_{obs.} - (r_{M-X})_{Pauling-Huggins}$

b  $(r_{M-X})_{obs.} - (r_{M-X})_{Schomaker-Stevenson}$

Table XII

Bond Angles

	I	Br	Cl
Sb	99° 0.24 <sup>a</sup>	97° 0.14	96° 0.08
As	101° 0.36	100.5° 0.31	99° 0.30
P	102° 0.52	101.5° 0.53	100.5° 0.47

a  $(r_{X-X})_{Van\ der\ Waals} - (r_{X-X})_{obs.}$

Table XIII

Temperature Factor Exponents

	I	Br	Cl
Sb	0.003 215°C. <sup>a</sup>	0.003 115°C.	(0.004) 165°C.
As	0.004 190°C.	0.004 65°C.	0.003 30°C.
P	< 0.000 165°C.	< 0.001 65°C.	0.001 20°C.

a The temperature of the vapor as estimated from the heating current in the high temperature nozzle; subject to considerable uncertainty.

## A Discrepancy Between Long and Short Camera Pictures

A serious discrepancy between the diffraction photographs of antimony triiodide taken with the long and the short camera lengths has been discovered.  $s_o = \frac{4\pi}{\lambda} \sin \frac{\phi}{2}$  for a given feature should be the same for both lengths. Table XIV shows an average disagreement of 2.6% with the long camera rings relatively too small. The error might arise in at least six ways.

1). Film shrinkage.--Drying of the film in the high vacuum of the apparatus might cause a temporary shrinkage that would make the rings too large when the film was developed. Measurements on the shadows of fiducial marks in the apparatus show an isotropic shrinkage of about 1/2 to 1%. This shrinkage should affect the long and short camera pictures and the calibration pictures of gold foil to the same extent.

2). Incorrect settings of the comparator pointers.--Due particularly to the background scattering it is difficult to pick the exact position of a given feature. Individual measurements generally show deviations of about 1% or less, depending on the observer, due to this uncertainty. The averages of the measurements for the various features generally show better agreement. However there may be a general tendency to measure all rings too large or too small. For example a tendency to get measurements about 1/2% larger on dense photographs than on light ones is often observed. I tried setting the pointers on the long camera pictures at the diameter each feature should have as calculated from the short camera pictures. The setting thus determined always appeared far larger than the actual diameter of the ring could possibly be, according to the present methods of interpretation.

3). Incorrect measurement of the camera length.--If one or both of the measured camera lengths (which together with the ring diameters determine  $\phi$ ) was in error, the discrepancy might be explained. However this is very unlikely due to the rigid con-

structure of the apparatus which keeps the lengths constant to less than 0.3%

4). Incorrect value of  $\lambda$ .--While doubt has been raised as to the validity of calibrating  $\lambda$  from gold foil pictures, there is no apparent reason why the value should change from one set of pictures to the next.  $\lambda$  is dependent only on the accelerating voltage. This is checked at a constant value by a voltage divider and potentiometer in parallel with the apparatus. An accidental incorrect setting of the potentiometer is possible but very unlikely. Work on methods of calibrating electronic wave lengths with zinc oxide is now in progress in These Laboratories.

5). Magnetic fields in the apparatus.--The presence of a magnetic field within the camera end of the apparatus would cause the electrons to move in curved paths so that  $\phi$  could not be determined correctly from the ring diameters. Some steel screws and other parts in the camera might well have become magnetized. We have suspected the presence of a field for some time because the rings often show a slight ellipticity (1 or 2%).

6). Electrostatic fields.--An accumulation of charge from the central electron beam striking the non-conducting film would cause the scattered electrons to swerve toward or away from the center, depending on the sign of the charge, as they approached the film. For a given ring, the effect would be proportionally greater on the short camera pictures where the rings are nearer to the central image. Dr. Schomaker has checked the effect on  $CCl_4$  pictures, finding a 0.3% increase in ring diameter for the short camera length. His method of eliminating the field was to cut away the center of the film so that the central beam was conducted away by the metal film holder.  $CCl_4$ , however, did not show a discrepancy between long and short camera pictures. It is possible that compounds which show the disrecrepancy also have a greater electrostatic effect than  $CCl_4$  due to changes in the film resulting from surface contamination by the substance.

A reinvestigation of antimony triiodide.--A complete new set of pictures of antimony triiodide with both long and short camera lengths was taken about two years after the initial set. Special

care was taken to avoid errors (1). (2). (3), and (4). The discrepancy in this set was 1.7% (Table XIV).

Additional pictures were taken with an iron shield in the camera to neutralize any magnetic field. The shielding reduced the ring diameters of short and long camera pictures an average of 0.1% and 0.3% respectively (Table XV). Gold foil pictures show that the shield greatly reduced the ellipticity of rings. The effect of this shielding is receiving further study.

The new pictures were compared with the first set (Table XVI). The deviations were 0.6% for the short camera and 1.0% for the long camera lengths. This seems to be rather poor agreement in the latter case, suggesting that the long camera pictures are the ones in error.

Comparison with other compounds.--One would expect the six suggested explanations to apply equally to the photographs of all compounds. Unfortunately, few substances have been photographed at both distances. What little data there is indicates that the discrepancy varies from compound to compound or from time to time. Phosphorus trichloride, quinone, and a confidential substance show insignificant discrepancies. Dibromobutane pictures had a discrepancy of 1.5%. Attention is called to the results of quinone which show no significant discrepancy although quinone and antimony triiodide were studied by the same investigator under similar conditions.

Table XIV

Discrepancy Between  
Short and Long Camera

Max.	Min.	$s_{\text{short}} - s_{\text{long}}$		$s_{\text{unshielded}} - s_{\text{shielded}}$	
		old pictures	new pictures	short camera	long camera
3	3	3.7%	2.9%	-0.3%	0.1%
3	4	3.7	2.8	.0	-.2
4	4	2.6			
4	5	2.8			
5	5	2.7			
5	6	2.2	0.7	.0	-.2
6	6	2.1	1.2	.4	.5
6	(3.0)	(3.0)	2.7	.2	.6
7	7	2.2	1.4	.0	.5
7	8	1.8	1.3	-.6	.2
8	8	1.9	0.9	-.3	1.0
8	8	1.6	1.3	.1	0.1
average		2.6%	1.7%	0.1%	0.3%
ave. dev.		0.54%	0.77%	0.22%	0.36%

Table XV

Effect of Magnetic  
Shield for New Pictures

	$s_{\text{unshielded}} - s_{\text{shielded}}$
	s

Max.	Min.	old pictures	new pictures	short camera	long camera
3	3	3.7%	2.9%	-0.3%	0.1%
3	4	3.7	2.8	.0	-.2
4	4	2.6			
4	5	2.8			
5	5	2.7			
5	6	2.2	0.7	.0	-.2
6	6	2.1	1.2	.4	.5
6	(3.0)	(3.0)	2.7	.2	.6
7	7	2.2	1.4	.0	.5
7	8	1.8	1.3	-.6	.2
8	8	1.9	0.9	-.3	1.0
8	8	1.6	1.3	.1	0.1
average		2.6%	1.7%	0.1%	0.3%
ave. dev.		0.54%	0.77%	0.22%	0.36%

Table XVI  
Discrepancy Between New and Old Pictures

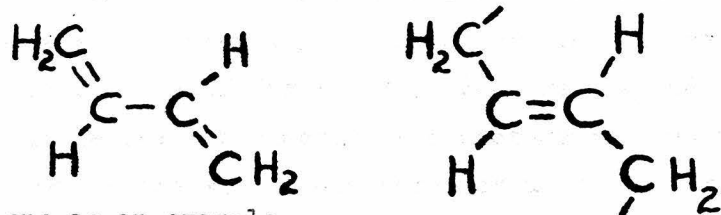
Max.	Min.	$s_{\text{new}} - s_{\text{old}}$	
		s	short camera
3	3	1.6%	1.7%
3	4	-0.4	0.3
4	4		
4	5		
5	5	1.1	1.7
5	6	0.0	1.1
6	6	1.0	0.9
6	7	-0.4	(-0.1)
7	7	1.1	(1.3)
7	8	-0.1	1.0
8	8	1.2	1.5
average		0.6%	1.0%
ave. dev.		0.7%	0.47%

#### Discussion

The discrepancy between long and short camera pictures remains unexplained. None of the six suggestions apparently accounts for it. It may be that the accuracy of current methods of measuring electron diffraction photographs should be checked with artificial photographs or by other means. Also, a variety of compounds should be reinvestigated at both camera distances to determine in what cases there is a serious discrepancy. The electrostatic effect in particular and perhaps the magnetic effect should receive further study in the case of compounds which consistently show a discrepancy. Until this work is completed the accuracy of electron diffraction investigations in general is subject to question.

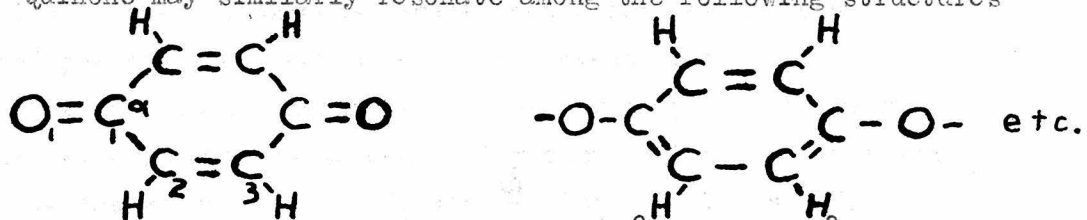
### The Structure of Quinone

Quinone in the vapor state has been found in this investigation to have a structure such as would be expected for a conjugated molecule rather than the anomalous structure reported for crystalline quinone (29). A reasonable structure for quinone can be predicted by a consideration of the bond lengths in related molecules. C - C single bonds in unconjugated molecules generally have a length of 1.54 Å. On the other hand 1.44 Å. to 1.48 Å. has been found by electron diffraction in butadiene 1-3, cyclopentadiene, glyoxal, dimethylglyoxal, stilbene (x-ray diffraction) and other conjugated molecules. Furthermore these molecules exhibit restricted rotation about the single bonds indicating partial double bond character. An explanation of these characteristics of conjugated molecules is afforded by assuming resonance among structures such as



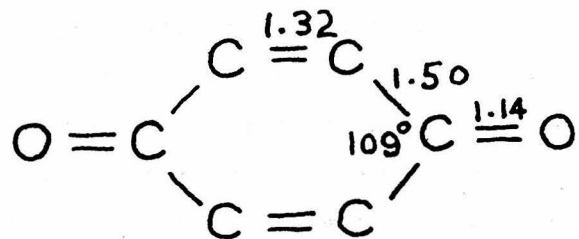
for butadiene as an example.

Quinone may similarly resonate among the following structures



We would expect  $C_1 - C_2$  to be between 1.54 Å. and 1.39 Å., the respective values for single bonds and 50% double bonds, probably somewhat nearer the former value. Angle  $\alpha$  should be slightly less than  $120^\circ$  as found for benzene but greater than the tetrahedral value,  $109^\circ$ . For the C = O bond we might expect a length near 1.20 Å., the value reported for glyoxal.

In studying crystalline quinone by x-ray diffraction Robertson (25) found the following structure:



His values for C = O and the angles seem unlikely. I am presenting in this paper the results of an electron diffraction investigation of the structure of vaporized quinone.

Experimental.--Eastman white label quinone was used in the investigation without additional purification. Diffraction photographs were prepared with camera lengths of 10.75 cm. and 20.15 cm. The appearance of the photographs exclusive of background and the gradual decrease in intensity of the outer rings is represented by the broken line curve of figure (7). Features beyond the ninth maximum could be seen on superimposed photographs but their exact shapes were quite indistinct and were not used in picking the correct structure. Dr. Schomaker and I agree closely on the details of the photographs except that I can see no details beyond the ninth maximum except the eleventh maximum.

The diffraction patterns were measured by one observer. About ten measurements were made for each feature and averaged to give the values of  $q_0 = \frac{10}{\lambda} \sin \frac{\Phi}{2}$  listed in Table XIX. It should be noted that the long and short camera pictures are in good agreement (See discussion in previous paper). In this case  $q_0 = \frac{10}{\lambda} S_0$  was used in the calculations in order to use the I.B.M. calculators for the theoretical intensity curves.

A radial distribution function (eq. 3) was evaluated and plotted in fig. (7). In principle this summation curve, or preferably the integral (30) is sufficient for determining the structure, and theoretical intensity curves are unnecessary. The simplest procedure

in analyzing radial distributions is to select isolated peaks which by themselves determine some interatomic distance. If enough isolated peaks are not present an attempt is sometimes made to estimate the positions of component parts of unresolved peaks or to find a combination of interatomic distances which would add together to give the observed radial distribution. In the case of quinone, very little use was made of the radial distribution.

In determining the structure of quinone, the molecule was assumed to be planar, and no attempt was made to determine the length or angle of the C - H bond. With these simplifications, the determination was a four parameter problem. For convenience these parameters may be  $C_2 = C_3$ ,  $C_1 - C_2$ ,  $C_1 = O_1$ , and  $\alpha$ . Many other combinations of four interatomic distances could be used as the parameters, of course, or as was actually done, the distances  $C_2 = C_3 = 1.34 \text{ \AA}$ . and  $C_2 - H_1 = 1.08 \text{ \AA}$ . were assumed for all models, and the fourth parameter was a factor which multiplied all the distances in the assumed models to give the actual distances.

In applying the usual correlation method to quinone, theoretical intensity functions (eq. 2) of the form

$$I \propto \sum_{m \neq m'} \frac{Z_m Z_{m'}}{r_{m-m'}} \sin(\alpha r_{m-m'}) \quad (5)$$

summed over all pairs of atoms in the molecule were evaluated for various models.  $C_2 = C_3$  was taken as  $1.34 \text{ \AA}$ . in all cases. Five series of calculations were made for  $C_1 - C_2 = 1.54, 1.52, 1.50, 1.48$ , and  $1.46 \text{ \AA}$ . respectively. A few additional calculations at  $1.44 \text{ \AA}$ . and  $1.42 \text{ \AA}$ . were made. For each of these series,  $C = 0$  was varied from about  $1.18 \text{ \AA}$  to  $1.28 \text{ \AA}$  in steps of  $0.04 \text{ \AA}$  and  $\alpha$  was varied from  $112^\circ$  to  $120^\circ$  in increments of about  $3^\circ$ . The extent of qualitative agreement of each of these theoretical curves with the observed scattering distribution is indicated in Tables XVII. In many cases the appearance of additional curves was estimated by extrapolation or interpolation of the calculated values (indicated by parentheses in the same tables). Additional calculations were made for intermediate models that showed promise of being correct

or nearly so. The curve for the best model in each set having a particular value of the  $C_1 - C_2$  distance and in some cases also curves for neighboring models are shown in fig. (7). The models selected are designated by numbers I to X in Table XVII. Table XVIII gives the values of the parameters assumed for these models.

Table XVIII

Model	$C = C$	$C - C$	$C = O$	$\alpha$
I	1.34	1.54	1.30	116°
II	1.34	1.52	1.24	117°
III	1.34	1.50	1.24	116°
IV	1.34	1.50	1.24	117°
V	1.34	1.48	1.22	115°
VI	1.34	1.48	1.22	116°
VII	1.34	1.48	1.20	118°
VIII	1.34	1.48	1.22	118°
IX	1.34	1.48	1.24	118°
X	1.34	1.46	1.20	116°

An estimate of the sensitivity of the shape of the curve for variations in the parameters can be made by comparing curves V, VI, and VIII and curves VII, VIII, IX. Models I, II, and X are considered distinctly inferior to the others. VII and IX are slightly inferior.  $\frac{q}{q_0}$  values for the important features of the best seven of these curves are listed in Table XIX. From the average weighted ratio of  $q/q_0$  for each model the corresponding interatomic distances were readjusted giving the values in Table XX. The readjusted parameters are nearly the same for all the satisfactory models giving as the final result  $C_1 - C_2 = 1.48 \text{ \AA.} \pm 0.03 \text{ \AA.}$ ,  $C_2 = C_3 = 1.33 \text{ \AA.} \pm 0.02 \text{ \AA.}$ ,  $C_1 = O_1 = 1.22 \text{ \AA.} \pm 0.03 \text{ \AA.}$ , and  $\alpha = 116^\circ \pm 2^\circ$ . These values agree well with our initial predictions.

Table XVII

The Degree of Qualitative Agreement Between the Observed  
Scattering Curve and Curves for Various Models

$$C_1 = C_2 = 1.18 \text{ \AA} \quad 1.20 \text{ \AA} \quad 1.22 \text{ \AA} \quad 1.24 \text{ \AA} \quad 1.26 \text{ \AA} \quad 1.28 \text{ \AA}$$
$$C_1 - C_2 = 1.54 \text{ \AA}$$

$\alpha$	$C = O$	1.18	1.20	1.22	1.24	1.26	1.28	1.30
110°			D					
112°			C			(C)		
113°			C	(C)		B	C	C
116°	D		C	(C)	B	(B)		$B_I$
118°	C	(C)	B	(B)	B			(C)
120°			C	C	C	C		
122°			C					

- A Excellent qualitative agreement; within the limits of error.
- B Fairly good agreement but definitely not the best.
- C Very poor agreement, only faintly resembling the appearance of the photographs.
- D Shows practically no similarity.
- ( ) Extrapolated or interpolated.

Table XVII cont.

$$C_1 - C_2 = 1.52 \text{ \AA.}$$

$C = 0$	1.18	1.20	1.22	1.24	1.26	1.28
$\alpha$						
113°		B		B	(B)	(C)
115°				B <sup>+</sup>	A <sup>-</sup>	
116°	D		B	A <sup>-</sup>	A <sup>-</sup>	(B)
117°			(B)	A <sup>-</sup> <sub>II</sub>	A <sup>-</sup>	(B)
118°		B	(B)	A <sup>-</sup>	(A <sup>-</sup> )	B

Table XVII cont.

$$C_1 - C_2 = 1.50 \text{ \AA.}$$

113°	(C)	B	(B <sup>+</sup> )	B	
115°			(A <sup>-</sup> )	A <sup>-</sup>	(A <sup>-</sup> )
116°	B	(B)	A <sup>-</sup>	A <sup>+</sup> <sub>III</sub>	A <sup>-</sup>
117°		(B)	A	A <sup>+</sup> <sub>IV</sub>	(A <sup>-</sup> )
118°			(A <sup>-</sup> )	A <sup>-</sup>	
120°				(B)	

Table XVII cont.

$$C_1 - C_2 = 1.48 \text{ \AA.}$$

	$C = 0$	1.16	1.18	1.20	1.22	1.24	1.26	1.28
$\alpha$								
113°				B	$A^-$	B		
115°				B	$A_V^+$	$A^-$		
116°		(B)		$A^-$	$A_{VI}^+$	$A^-$	(B)	
118°		(C)		$B_{VII}$	$A_{VIII}^+$	$A_{IX}^+$		B
120°				B	B	$A^-$		

Table XVII concl'd.

$$C_1 - C_2 = 1.46 \text{ \AA.}$$

112°	C	$B^+$	(C)
116°	D	$B_X$	C
118°	C	B	B

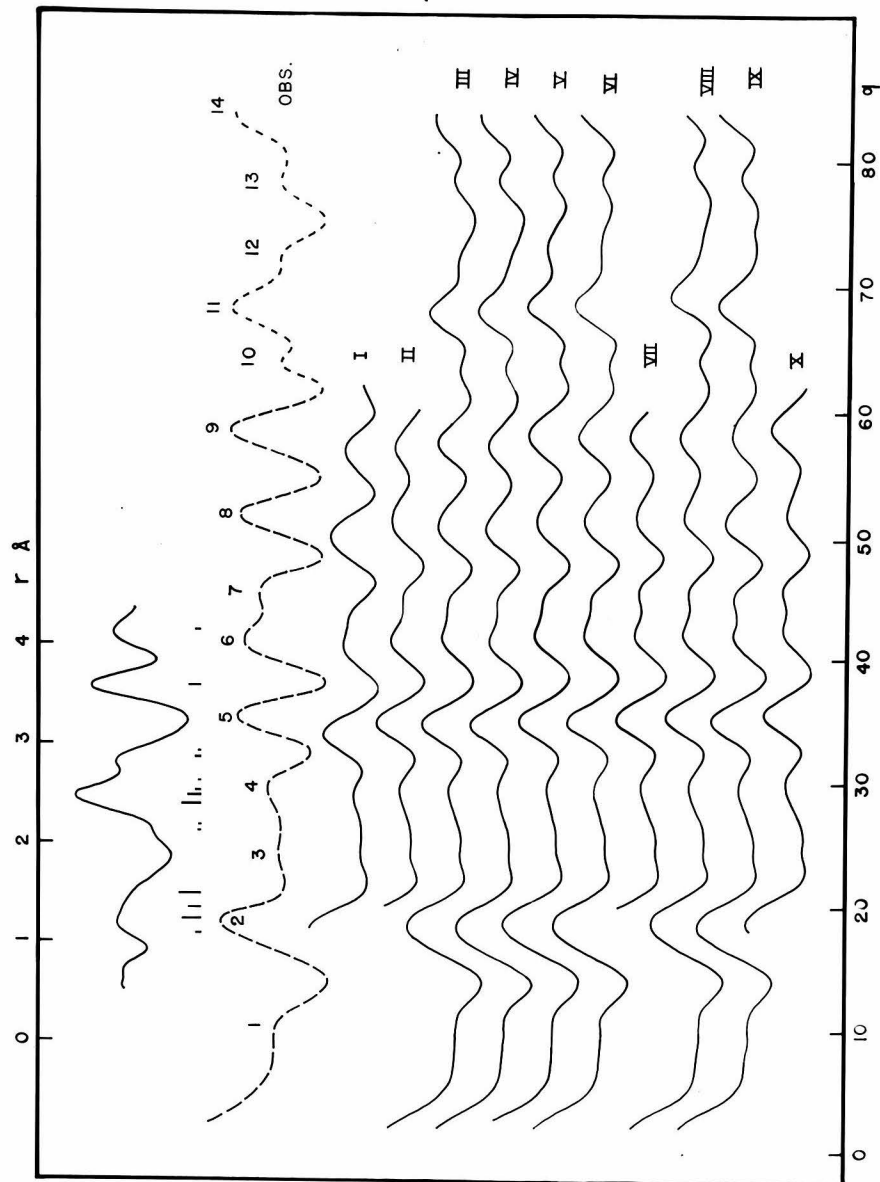


Figure 7  
Quinone. Radial distribution summation (upper)  
and intensity curves.

Max.	Min.	$q_k$	$q_0$	II	III	IV	V	VI	VII	VIII	IX
1	2	-14	10.57								
		8	13.84								
2	2	18	17.70								
		-11	21.70								
3	4	10	24.22								
		-12	26.66								
4	4	12	29.67	(.988)	(.978)	(.999)	(.998)	(.995)	(1.000)	(0.994)	
		-18	32.4	.981	.974	.979	.985	.991	0.996	.988	
5	5	20	35.2	.986*	.986*	.986*	.994*	.995*	1.002*	.997*	
		6	-16	38.0	1.002*	1.002*	1.008*	1.012*	1.012*	1.018*	
6	6	10	41.2	1.004	1.016	1.010	1.023	1.023	1.018	1.020	
		7	-6	43.4	(1.000)	(0.998)	(0.994)	(1.012)	(1.006)	(1.019)	(0.996)
7	7	7	45.7	(0.985)	(.974)	(.976)	(0.996)	(0.976)	(0.994)	(0.982)	
		8	-15	48.2	.984*	.981*	.980*	.981*	.988*	1.000*	.991*
8	9	9	51.6	.990*	.990*	.990*	.990*	.990*	.996*	.988*	
		-8	54.6	.996	.995	.991	1.006	1.001	1.008	1.001	
9	9	6	58.3	.998	.986	.983	.997	.994	0.996	0.996	
		Average	0.990	0.988	0.989	0.998	0.998	0.998	1.004	1.000	0.0082
		Ave. dev.	0.0071	0.0094	0.0096	0.0096	0.0091	0.0091	0.0101	0.0101	

Table XX

Final Results

Model	$\alpha$	$C = C$	$C - C$	$C = O$	Ave. dev.	Comments
II	$117^\circ$	1.325	1.505	1.23	0.0071	inferior
III	$116^\circ$	1.320	1.48	1.225	.0094	good
IV	$117^\circ$	1.325	1.48	1.225	.0096	good
V	$115^\circ$	1.335	1.48	1.22	.0096	good
VI	$116^\circ$	1.335	1.48	1.22	.0091	good
VIII	$118^\circ$	1.345	1.49	1.225	.0082	sl. inferior
IX	$118^\circ$	1.340	1.48	1.24	.0101	sl. inferior

Report  $116^\circ \pm 2^\circ$   $1.33 \pm .02$   $1.48 \pm .03$   $1.22 \pm .03$

References

1. L. O. Brockway, Rev. Modern Physics, 8, 231 (1936)
2. P. Debye, Ann. d. Physik, 46, 809 (1915)
3. H. Mark and R. Wierl, Naturwissenschaften, 18, 205, 778 (1930)
4. R. Wierl, Ann. Physik, 8, 521 (1931), 13, 453 (1932)
5. H. Bethe, Ann. Physik, 87, 55 (1928), 5, 325 (1930)
6. N. F. Mott, Proc. Cambridge Phil. Soc., 25, 304 (1929)
7. L. Pauling and L. O. Brockway, J. Chem. Phys., 2, 867 (1934)
8. L. Pauling and L. O. Brockway, J. Am. Chem. Soc., 57, 2684 (1935)
9. V. Schomaker, Thesis C.I.T. 1938
10. L. Pauling and M. L. Huggins, Z. Krist., 87, 205 (1934)
11. L. Pauling, "The Nature of the Chemical Bond", Cornell Univ. Press, Ithaca, N. Y.
12. V. Schomaker and D. P. Stevenson, J. Am. Chem. Soc., 63, 37 (1941)
13. L. O. Brockway and F. T. Wall, J. Am. Chem. Soc., 56, 2373 (1934)
14. A. H. Gregg, G. C. Hampson, G. I. Jenkins, L. F. Jones, and L. E. Sutton, Trans. Far. Soc., 33, 852 (1937)
15. O. Hassel and A. Sandbo, Z. Phys. Chem., B41, 75 (1938)
16. L. O. Brockway and H. O. Jenkins, J. Am. Chem. Soc., 58, 2036 (1936)
17. H. D. Springall and L. O. Brockway, ibid., 60, 996 (1938)
18. L. O. Brockway, ibid., 57, 958 (1935)
19. L. O. Brockway, Proc. Nat. Acad. Sci., 19, 303 (1933)
20. L. O. Brockway, J. Phys. Chem., 41, 185, 747 (1937)
21. See M. W. Lister and L. E. Sutton, Trans. Far. Soc., 37, 393 (1941), for a revision of the estimated errors.
22. E. H. Eyster, J. Chem. Phys., 6, 580 (1938)
23. L. Pauling, H. D. Springall, K. J. Palmer, J. A. C. S., 61 927 (1939)
24. L. O. Brockway and J. M. Robertson, J. Chem. Soc., 1324 (1939)
25. V. Schomaker and R. Spurr, J. Am. Chem. Soc., 64, 1184 (1942)
26. V. Schomaker and D. P. Stevenson, To be published.
27. Chr. Finbak and O. Hassel, Z. Phys. Chem., B39, 471 (1938)
28. See R. W. Spitzer, W. J. Howell, Jr., and V. Schomaker, J. Am. Chem. Soc., 64, 62 (1942) for an earlier application of this procedure.

29. J. M. Robertson, Proc. Roy. Soc., 150, 106 (1935)
30. R. Spurr and W. Shand, J. Am. Chem. Soc., 65, 179 (1943)

Part II  
Precipitation Reactions Between Antibodies  
and Benzoic Acid Derivatives

## Part II

### Precipitation Reactions Between Antibodies and Benzoic Acid Derivatives

#### A. Qualitative

Biological reactions are generally too complicated to be studied readily from a chemical point of view. In most cases the exact nature of the reactants and the products is unknown. Often even the number of components involved in the reacting system has not been determined. The study of simplified chemical reactions closely related to the more complex natural ones is a promising approach to the solution of many biological problems. I am presenting here the results of one of several investigations of the reactions of antibodies with relatively simple organic molecules. It is believed that these reactions are closely related to the complicated phenomenon of acquired immunity to disease and to other important biological phenomena.

When a foreign substance of certain types, such as proteins or bacterial cells, is introduced into the blood stream of an animal, (e.g. by injection) the animal responds by producing a specialized protein, called an antibody, which appears in the blood. The foreign substance which stimulates the antibody production is called an antigen. When corresponding antigens and antibodies are mixed *in vitro* under suitable conditions they combine with the formation of a precipitate (the precipitin reaction). The reaction is highly specific in that a given antibody will combine only with the antigen that produced it or with other test antigens containing some of the same chemical groups as those in the injected or immunizing antigen. It is believed that the antibody and antigen molecules have complementary configurations which cause this highly specific combination. A detailed explanation of the nature of the bonding or an extensive review of the literature on the subject is beyond the scope of this thesis.

Natural antigens are too complicated to give much information about the precipitin reaction. Landsteiner and van der Scheer (1) introduced a simplification by using as antigens azoproteins carrying various characteristic organic molecules (called haptens) coupled to

the protein by an azo linkage. They found that any suitable protein carrying the same characteristic hapten as was present on the azo-protein antigen will give a good precipitin reaction with the corresponding antibody. Thus, the reaction shows specificity for the known structure of the hapten. The unknown protein structure is of less importance.

Landsteiner and van der Scheer found later (2) that many azo-dyes containing the same hapten as the immunizing antigen also gave good precipitates. Pauling and coworkers (3) investigated several simple compounds containing phenylarsonic acid as the hapten. They obtained precipitates with all of these substances which contained two or more haptenic groups widely separated in the molecule. No monohaptenic dyes gave precipitates, presumably due to their inability to combine with two antibody molecules and join them together in the framework that makes up the precipitate. In the case of antigens having two hapten groups very close together it is probable that a second antibody molecule cannot combine with the antigen because of steric interaction with the first antibody molecule that combines. Hooker and Boyd (10), on the other hand, were unable to get reactions with benzoic acid azo dyes although azoproteins carrying this hapten reacted well. Since there was no apparent reason on the basis of the framework theory of precipitation (4) why dyes with phenylarsonic acid should be effective when benzoic acid dyes are not, it seemed worthwhile to extend the investigations. A qualitative study of the precipitin reaction for six p-amino benzoic acid derivatives is presented here. The experiments show that precipitates can be obtained with certain types of simple benzoic acid compounds.

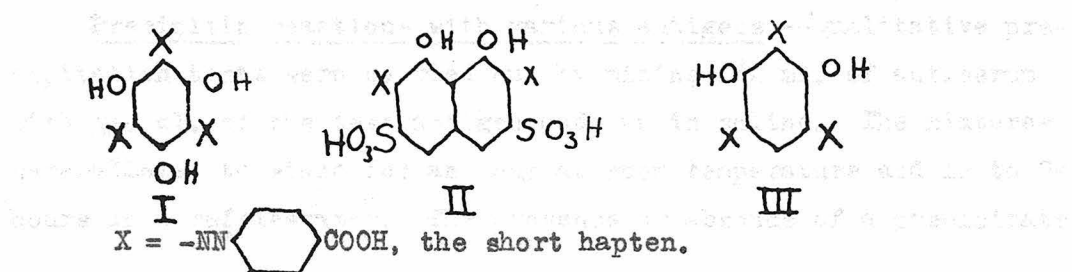
An outline of the experiment.--Rabbits were immunized by injections of an azoprotein made from beef serum and p-aminobenzoic acid. The titer was checked with a test antigen made from ovalbumin and p-aminobenzoic acid. The various simple p-aminobenzoic acid derivatives were tested with the high titer serum to determine which ones gave a precipitin reaction.

Immunizing antigen.--Diazotized p-aminobenzoic acid coupled with beef serum by the method of Landsteiner and van der Scheer (5) was used for inoculating the rabbits. Two preparations were made with 0.9 g. and 1.8 g. respectively of p-aminobenzoic acid coupled to 200 ml. of serum and made up to 600 ml. They were used interchangeably after it was found that they gave rise to antisera of similar titer.

Azo-ovalbumin test antigen.--One gram of p-aminobenzoic acid was diazotized and coupled with a solution of 2 g. of crystalline ovalbumin kept at pH 8 with sodium carbonate during the coupling. I am indebted to Mr. Carol Ikeda for this preparation. For preparing these two azoproteins, p-aminobenzoic acid was diazotized in a hydrochloric acid solution at 0° C. by adding sodium nitrite to the starch-iodide end-point.

Preparation of antiserum.--Eight rabbits were injected intraperitoneally or intravenously with 1/2 to 1 ml. portions of the immunizing antigen. For several months they received courses of injections given daily for a week followed by rest for a week. Thereafter they were injected only three or four times each week on alternate days. Every month or two the rabbits were bled from the ear on the eighth, ninth, and tenth days after the last injection, about 40 ml. generally being obtained on each day. The blood was allowed to clot causing the serum to separate. The antisera obtained were pooled according to the amount of precipitate small samples gave with the azo-ovalbumin test antigen. The first few batches of sera obtained were of relatively low titer. Only the sera obtained after nine months were used in these experiments.

Preparation of test antigens having short haptenic groups.--



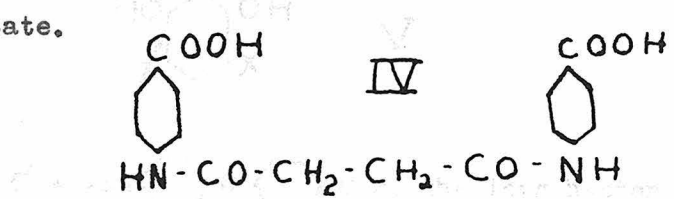
were prepared by coupling diazotized p-aminobenzoic acid (30% excess) with phloroglucinol, chromotropic acid, and resorcinol respectively. As the first step, the amount of p-aminobenzoic acid required for the synthesis was converted to the sodium salt by dissolving it in a sodium hydroxide solution. The theoretical amount of sodium nitrite for complete diazotization was added and the solution was poured rapidly into a mixture of excess hydrochloric acid and sufficient ice to keep the temperature near 0° C. A somewhat colored solution of the diazonium compound and a slight amount of precipitate were obtained. It was coupled to the appropriate nucleus about ten minutes after being mixed. The coupling reaction was allowed to proceed for one to three days in a solution kept at pH 8-9 with sodium carbonate. The product was precipitated with hydrochloric acid and purified by repeated solution in sodium hydroxide and precipitation with hydrochloric acid followed by thorough washing with acidified water. C, H analyses are given in Table I.

In basic solution the diazonium compound alone, without a nucleus with which to couple, gives rise to a large amount of highly colored brown material which behaves like the desired products in being soluble in base and insoluble in acid. Hence any test antigens prepared from diazotized p-aminobenzoic acid in the manner outlined may be expected to contain large amounts of this impurity, as was probably the case in antigens I and II. The impurity shows strong inhibition as will be discussed. The resorcinol compound (III), however, was extracted repeatedly with hot 80% alcohol which seemed to remove the impurity. The product was further treated with diazotized p-aminobenzoic acid to insure complete substitution and again purified.

Precipitin reactions with various antigens.--Qualitative precipitation tests were carried out by mixing 1/2 ml. of antiserum with 1/2 ml. of the test antigen made up in saline. The mixtures were allowed to stand for an hour at room temperature and 12 to 24 hours in a refrigerator. The presence or absence of a precipitate

was noted visually. The simple test antigens were generally used in concentrations from 1:10,000 to 1:270,000 in steps of three-fold dilution. The tests were tried repeatedly as the strength of the antiserum obtained increased.

Good precipitates were obtained in a few minutes with the azo-ovalbumin whereas controls with untreated ovalbumin gave no reaction. This indicates that benzoic acid is a satisfactory hapten when coupled to ovalbumin. Nevertheless none of the simple test antigens with short haptenic groups (compounds I, II, and III) gave a precipitate.



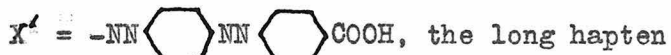
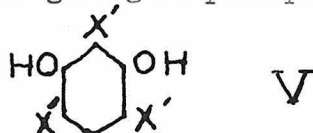
also failed to precipitate. Later it was found that these short antigens and also the brown impurity show strong inhibition for the precipitin reaction between other benzoic acid antigens and the antiserum.

The short resorcinol dye (compound III) was purified with alcohol as mentioned and tested at concentrations from 1:5,000 to 1:270,000 with the strongest serum obtained. Further tests at pH 6.0 were tried. In no case did precipitation occur. It seems unlikely that the amount of impurity present in the test antigen was sufficient to cause complete inhibition. Work on this type of dye was discontinued in favor of studies on test antigens having longer hapten groups.

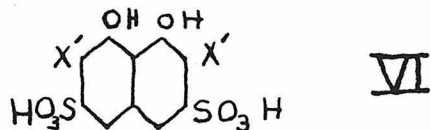
Preparation of the long hapten.--The long haptenic group referred to below, p-(p-aminophenylazo) benzoic acid,  $\text{H}_2\text{N}-\text{C}_6\text{H}_4-\text{N}_2-\text{C}_6\text{H}_4-\text{COOH}$  was made by coupling diazotized p-aminobenzoic acid with the theoretical amount of aniline-methyl-sulfonate (6) and hydrolyzing the product for 1 1/2 hours at 90° C. in 1N NaOH. The desired product was purified by precipitating it three times at pH 6, the brown impurity mentioned in the preparation of short antigens remaining in solution at this pH.

It was recrystallized twice from hot 80% alcohol as the sodium salt.

Test antigens containing the long haptenic group.--The long hapten was diazotized by the inverted procedure used for the short hapten, giving a gray-green to pink precipitate soluble in basic solutions. Coupling with a suitable nucleus was carried out in a basic solution (pH 8-9) as before. Here again the diazotized long hapten alone in basic solution produced an impurity, in this case a red dye which gave good precipitin reaction.



was prepared using resorcinol and a 30% excess of the diazotized hapten. The product gave a good precipitin reaction only after being dialyzed in a Visking bag for a week against water. It was found that the material contained two components, one soluble in salt solutions and the other insoluble in the 0.9% salt concentration used in the precipitin tests. Both components gave a definite precipitate with the antibody. Neither of the components was found to be identical with the red impurity as shown by the distinctly different colors they gave in concentrated sulfuric acid. It was decided not to use either component in further experiments until their compositions could be determined.



(the test antigen used in further experiments) was prepared with the theoretical amounts of chromotropic acid and the long diazonium compound in order to reduce the tendency to form the red impurity which is produced by an excess of the diazonium compound. As a result, considerable mono-substituted compound formed. This was

largely removed by repeated extraction with 80%-90% acetone saturated with salt. Without the salt the desired product also dissolved. This test antigen gave the best precipitin reaction of all the simple substances tried. Controls with normal serum showed no reaction.

### Precipitating Power of Simple Test Antigens (Qualitative )

analysis	precipitating power	calculated	found	antigen	
				calculated	found
II	none	56.8% 59.4%	3.16% 3.53%	C <sub>12</sub> H <sub>10</sub> N <sub>2</sub> O <sub>4</sub>	C <sub>12</sub> H <sub>10</sub> N <sub>2</sub> O <sub>4</sub>
I	none	59.7% 59.4%	3.58% 3.08%	C <sub>12</sub> H <sub>10</sub> N <sub>2</sub> O <sub>4</sub>	C <sub>12</sub> H <sub>10</sub> N <sub>2</sub> O <sub>4</sub>
III	none	46.7% 48.5%	2.62% 3.11%	C <sub>12</sub> H <sub>10</sub> N <sub>2</sub> O <sub>4</sub>	C <sub>12</sub> H <sub>10</sub> N <sub>2</sub> O <sub>4</sub>
III	none	58.8% a 60.3%	2.74% 3.26%	C <sub>12</sub> H <sub>10</sub> N <sub>2</sub> O <sub>4</sub>	C <sub>12</sub> H <sub>10</sub> N <sub>2</sub> O <sub>4</sub>
IV	none	58.9% b 59.0%	3.64% 3.56%	C <sub>12</sub> H <sub>10</sub> N <sub>2</sub> O <sub>4</sub>	C <sub>12</sub> H <sub>10</sub> N <sub>2</sub> O <sub>4</sub>
V	fair	61.3% d 63.0%	4.0% 3.87%	C <sub>12</sub> H <sub>10</sub> N <sub>2</sub> O <sub>4</sub>	C <sub>12</sub> H <sub>10</sub> N <sub>2</sub> O <sub>4</sub>
VI	good	52.5% e 53.5% 54.0%	2.8% 3.6% 4.1%	C <sub>12</sub> H <sub>10</sub> N <sub>2</sub> O <sub>4</sub>	C <sub>12</sub> H <sub>10</sub> N <sub>2</sub> O <sub>4</sub>
		X = NN  COOH			
		X' = NN  NN  COOH			

a Before special purification.

b After special purification.

#### c Salt-insoluble component.

#### **d Salt-soluble component.**

e There was also 6% ash. It was assumed in calculating C and H and the concentrations in later experiments that 6% of the dry preparation was an inert impurity.

#### Discussion of Qualitative Experiments

The results of these experiments are summarized in Table I. None of the simple derivatives of the short hapten gave precipitates whereas all the derivatives of the long hapten were effective. A possible explanation of the ineffectiveness of the short compounds is that the benzoic acid groups are so close together that steric interference prevents two antibody molecules from joining to the same test antigen. It is not apparent why steric forces would not interfere to the same extent with the reactions of the corresponding phenylarsonic acid derivatives and their antibody. Possibly the greater strength of the bond between the antibody and the arsionic group is sufficient to overcome the steric repulsion.

The possibility that the short test antigens contained considerable amounts of inhibiting impurities cannot be ignored. However I believe that compound III in the purified form was reasonably free from such impurities. A C, H analysis agrees better with the theoretical value for the tri- or di-substituted resorcinol than with the mono-substituted compound. Quantitative inhibition tests showed that compounds II and III are even more powerful inhibiting agents than the brown impurity (Table V) indicating that the preparations do not owe their inhibiting power to the impurity.

Analyses of the test antigens were made in order to determine the type of organic material.

Analyses:

Compound I

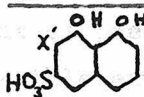
Compound II

Compound III

Quantitative and Qualitative Studies

Quantitative studies of the reaction between antiserum and the various benzoic acid derivatives were carried out to determine the effect of various conditions on the amount of precipitate obtained. The effects of pH, concentration of antigen, the presence of a different antiserum, and the presence of simple haptens were investigated. In special cases the molecular ratio of antigen to antibody in the precipitate was determined.

Materials used.--The antisera, the azo-ovalbumin test antigen and compound VI, the simple test antigen, were



those used in the qualitative studies. The purification of the simple haptens is mentioned later.

Formation and analysis of precipitates.--The appropriate reactants were mixed in a 0.9% saline solution generally buffered with borate (0.2M). The mixtures stood one hour at room temperature and overnight in a refrigerator. The precipitates were centrifuged and washed three times with 10 ml. portions of saline and finally transferred to clean tubes for analysis. The precipitates were dissolved in 0.5N NaOH. In some cases the test antigen content was determined colorimetrically with a Klett photoelectric colorimeter. Analyses for protein were made colorimetrically by the use of Folin-Ciocalteu (7) reagent. This technic has been found satisfactory in studies on phenyl arsonic acid antigens (8). The molecular weight of the antibody was taken as 160,000 in determining molecular ratios.

The effect of diluting the strong antiserum with a different antiserum.--In some preliminary experiments on hapten inhibition it was found desirable to dilute the strongest antiserum in order to reduce the amount of precipitate. The question was raised as to whether different diluting agents would give the same result. Three sets of quantitative precipitin tests were set up using the strongest antiserum (obtained from only one rabbit) diluted with antiovalbumin serum from rabbits, with saline, and undiluted respectively. The

concentrations of reactants in each tube and the results of the analyses are shown in Table II. A control with anti-ovalbumin serum but without the anti-benzoic acid serum was run at the higher test antigen concentrations. This control showed that a negligible amount of stable precipitate is brought down non-specifically from anti-ovalbumin serum by test antigen concentrations less than  $604 \times 10^{-6} M$ .

The anti-ovalbumin serum apparently strongly inhibited the precipitation in high test antigen concentrations, but increased the amount of precipitate somewhat in low test antigen concentrations. A possible explanation of these phenomena is being presented as a proposition. A larger proportion of dye was brought down in the system diluted with saline. A smaller proportion of the protein precipitated in the undiluted system, possibly due to the presence of borate buffer. Since these effects were incidental to the main purposes of this study, the experiments were not extended to other diluting agents, nor have definite conclusions been drawn.

The effect of pH on the amount and composition of the precipitate from antiserum and the simple test antigen.--Several series of tubes were set up in triplicate with 1 ml. each of an antiserum pool and of the simple dye test antigen (comp. VI) in borate buffered solutions at various pH values from 7.8 to 9.6. The antiserum pool used consisted of one part by volume of strong antiserum, three parts of weak antiserum, and 3/4 parts saline. The precipitates were analyzed for protein and for dye. The total protein precipitated and the antigen/antibody molecular ratio are recorded in Table III. The analyses are probably accurate to  $\pm 5\%$ , the ratios to  $\pm 10\%$ .

Two series of blanks were run at the same pH range. The first was set up with the antiserum present, but with the test antigen omitted. The second had anti-ovalbumin serum and the simple test antigen. Both blanks gave a negligible amount of precipitate. Controls were run with the simple test antigen added to a system of ovalbumin plus anti-ovalbumin serum. A negligible amount of dye was

Table II  
Antibodies in the Test Antigen and Antisera

Effect of Various Diluting Agents on Amount and Composition  
of Precipitate from Strongest Antiserum

		Dye dilution and concentration												
		a	1/500	1/1T	1/2T	1/4T	1/8T	1/16T	1/32T	1/64T	1/128T	1/256T	1/512T	1/1024T
diluent		b	986	580	299	145	72.5	36.2	18.1	9.06	4.53	2.27	1.13	0.57
		Composition of precipitate												
I		prot. <sup>c</sup>	52	0	0	6	51	136	189	245	230	138	33	10
Antioval.		dye <sup>d</sup>	-	-	-	-	1.1	1.7	2.2	2.8	2.8	2.2	-	-
		ratio <sup>e</sup>	-	-	-	-	3.9	2.4	2.3	2.2	2.4	3.1	-	-
II		prot.	0	27	108	241	315	270	239	199	160	25	2	0
Saline		dye	-	-	-	-	6.5	6.8	6.5	6.0	3.4	-	-	-
		ratio	-	-	-	-	4.0	4.9	5.3	5.9	4.1	-	-	-
III		$\frac{1}{10} \times$ prot. <sup>f</sup>	233	201	182	185	208	199	-	-	-	-	-	-
Undil.		dye ratio	36	23	17	15	15	12	-	-	-	-	-	-
IV		ratio	3.0	2.3	1.8	1.6	1.4	1.2	-	-	-	-	-	-
Control		prot.	26	2	0	-	-	-	-	-	-	-	-	-

- a. Dilution of test antigen before mixing.  
 b. Total test antigen concentration in mixture. M/liter  $\times 10^6$ .  
 c. Total protein in precipitate, Mg. antigen in ml. dilution.  
 d. Total antigen in precipitate, Mg.  
 e. Moles antigen / moles antibody in precipitate.  
 f. Total protein in precipitate  $\times 1/10$  for comparison.

- I 1/10 ml. antiserum, 9/10 ml. anti-oval., 1 ml. test antigen, pH 8.1.  
 II 1/10 ml. antiserum, 9/10 ml. saline, 1 ml. test antigen, pH 7.85.  
 III 1/2 ml. antiserum, 1 ml. test antigen in borate buffer, pH 8.1.  
 IV 1/2 ml. anti-oval., 1 ml. test antigen in borate buffer, pH 8.1

After each dilution, 1 ml. drop were run in borate buffer and dried at 100°. The diluted antigen oval well 1 ml. was washed 3 times of excess dilution. 1 ml. oval was added to each well and dried at 100°. After 10 min. the precipitate was washed 3 times with 1 ml. of borate buffer. The precipitate was dissolved in 1 ml. of 10% TCA.

brought down in the resulting ovalbumin-anti-ovalbumin precipitate. The optimum dye concentration was found to be about  $35 \times 10^{-6}$  M. (an initial dilution of 1/20 T). This is about the same concentration found by Pauling et al. (9) as the optimum for di-haptenic phenylarsonic acid dyes and the corresponding antiserum. The optimum is believed by these workers to be near the point where the antibody and the test antigen are present in equal molal concentrations. The optimum pH was about 9.0. Since the simple test antigen is probably completely ionized at all these pH values, it seems probable that the effect of hydrogen ion concentration is related in some way to its effect on the antibody molecules. In the corresponding phenylarsonic acid system the optimum pH has been found to be about 7.9 (9). Also borate buffer has a much more pronounced inhibiting action here than in phenylarsonic acid systems.

The antigen/antibody molecular ratios approached 1 at the lower test antigen concentrations and increased to about 2 at higher values. The ratio was not greatly dependent on the pH nor on the presence of borate buffer. A ratio of 1 or slightly more is expected for bivalent antigens and antibodies from the simple framework theory of precipitation (9). Values of about 1.3 have been found (9) for phenylarsonic acid dyes. The fact that ratios of 2 to 6 were found for the strongest antiserum (see previous section) suggests that the presence of this strong antiserum in these mixtures is responsible for the high ratios observed.

The effect of pH and borate buffer on the precipitation of antiserum by azo-protein test antigen.--Several series of tests at various pH values were set up in triplicate with 1 ml. of a diluted antiserum pool and 1 ml. of various concentrations of the azo-ovalbumin test antigen. Some were run with borate buffer and some without. The diluted antiserum pool was 1 part by volume of strong antiserum, 3 parts weak, and 8 parts saline or buffered saline. The total protein found in the precipitates is shown in Table IV.

The optimum pH was near 7.7 as compared with 9.0 for the simple test antigen. Also borate buffer had less effect here than before.

Table III

Effect of pH and Buffer on Amount and Composition of Precipitate from Antiserum and Simple Test Antigen

pH	a	Dye dilution and concentration					
		$\frac{1}{4T}$	$\frac{1}{8T}$	$\frac{1}{16T}$	$\frac{1}{32T}$	$\frac{1}{64T}$	$\frac{1}{128T}$
b	145	72.5	36.2	18.1	9.06	4.53	
Composition of precipitate							
borate 7.8	prot. <sup>c</sup> ratio	653 2.2	718 1.8	805 2.2	757 1.4	385 1.4	40 -
borate 8.1	prot. ratio	894 2.2	911 1.8	914 1.6	884 1.4	482 1.2	53 -
borate 8.4	prot. ratio	926 2.2	952 1.9	995 1.7	902 1.6	453 1.5	33 -
borate 8.8	prot. ratio	923 2.4	977 2.1	1012 1.9	983 1.7	519 1.8	56 -
borate 9.1	prot. ratio	913 2.2	964 1.9	1042 1.8	984 1.4	535 1.4	56 -
borate 9.2	prot. ratio	748 2.4	837 2.1	875 2.0	879 1.9	468 1.7	41 -
borate 9.6	prot. ratio	201 2.7	301 2.4	400 2.2	434 2.0	185 2.1	8 -
saline 8.1	prot. ratio	1087 2.7	1124 2.3	1143 1.9	1017 1.8	558 1.7	71 -

a Dilution of test antigen before mixing.

b Total test antigen concentration in mixture, M/liter  $\times 10^6$ .

c Total protein in precipitate,  $\mu$ g.

d Moles antigen / moles antibody in precipitate.

All tests contained 1 ml. dilute antiserum pool + 1 ml. simple test antigen diluted in borate buffered saline or unbuffered saline.

Table IV

The Effect of pH and Borate Buffer on the Amount of Precipitate from Antiserum and Azo-protein Test Antigen

pH	Test antigen dilution				
	$\frac{1}{36}$	$\frac{1}{54}$	$\frac{1}{81}$	$\frac{1}{121}$	$\frac{1}{182}$
<i>μg. protein in precipitate</i>					
6.5 <sup>a</sup>	(350)	(610)	(592)	(394)	(244)
6.5 <sup>b</sup>	230	529	549	412	241
7.15 <sup>a</sup>	310	536	664	486	288
7.25 <sup>b</sup>	172	561	665	539	381
7.5 <sup>a</sup>	329	659	700	520	365
7.75 <sup>a</sup>	416	682	742	598	429
7.9 <sup>a</sup>	340	600	666	565	386
8.0 to 8.2 <sup>a</sup>	316	616	681	574	382
8.05 <sup>b</sup>	211	535	605	530	365
8.35 <sup>a</sup>	152	536	604	548	361
8.9 <sup>b</sup>	6	448	586	474	328

a Antigen and antiserum diluted with saline.

b Antigen and antiserum diluted with buffered saline.

All tests contained 1 ml. diluted antiserum pool plus 1 ml. diluted azo-protein test antigen.

The effect of simple haptens on the amount of precipitate.

It might be expected that benzoic acid derivatives or structurally similar compounds smaller than the test antigen used would react with the antibody even though they did not give a precipitate. If these simple haptens were added to the antibody-antigen system, a decrease in the amount of precipitate would be expected. This phenomenon has been observed in many cases (5,8,9,11, and 12). A quantitative study of the relative inhibiting powers of various similar haptens gives insight into the nature of the bonding of the haptens to the antibody.

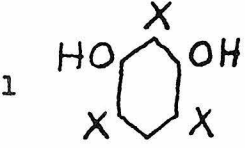
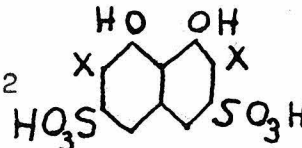
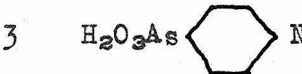
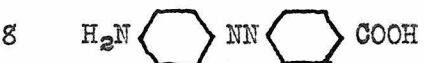
A wide selection of benzoic acid derivatives and related compounds are readily available. We selected sixty-three simple haptens for study. These were recrystallized from suitable solvents if necessary until the melting points were within one degree of the temperature recorded in the literature. Tests were set up in triplicate with 1 ml. portions each of antiserum pool, hapten solution, and test antigen solution. The antiserum pool was the same as that used in the pH experiments (1 part by volume of buffered strong antiserum, 3 parts weak, and 0.75 parts buffered saline). The simple test antigen was added at a concentration of 1 to 18,000. The haptens were at concentrations of  $150 \times 10^{-6}$  M,  $50 \times 10^{-6}$  M, and  $16.7 \times 10^{-6}$  M. All reactants were buffered, giving a pH of 8.6 to 8.7. The precipitates were analyzed for total protein. Forty-two of the haptens did not give sufficient inhibition at these concentrations. They were tested further at 0.01 M, 0.002 M and 0.004 M concentrations. Controls were run with no hapten present to give a basis for comparing the relative inhibiting powers. The percentage by which the precipitation was inhibited by each hapten at each concentration was calculated and recorded in Table V, which is arranged in the order of decreasing inhibition. In five cases (designated by \*) the tests were repeated to check on peculiar results of the first set. Only the new values are given in these cases.

A constant  $K_a$  (Table V) representing the relative inhibiting

power was calculated for each hapten on the basis of the percentage inhibition.  $p\text{-CH}_3$ (benzoic acid)(25% inhibition at  $50 \times 10^{-6}$  M) was used as the reference point with  $K_a$  assigned the value of 1.0. This compound was selected because it was intermediate in the scale of inhibiting powers and showed no peculiarities. The percentage inhibition of other compounds at the same concentration was multiplied by  $1.0/25 = .04$  to determine their constants. The constants at  $16.7 \times 10^{-6}$  M concentration was determined by multiplying the corresponding percentage inhibition by .074, this being the number which gave most of the haptens about the same constant at  $16.7 \times 10^{-6}$  M as they had at  $50 \times 10^{-6}$  M. In a similar manner constants were determined at the other concentrations. An average constant for each hapten is given in Table V. Greater weight was given to the values of inhibition between 15% and 85% where possible. The constants thus determined are only approximate. It is apparent from the table that in many cases the order of relative inhibiting power of two substances is reversed in different concentrations. In all such cases both substances were assigned the same constant.

The entire series of inhibition tests was repeated with the azo-ovalbumin test antigen at a dilution of 1 to 60 instead of the simple test antigen. The percentage inhibition in each case is recorded immediately below the corresponding values for the simple test antigen. A relative constant ( $K_b$ ) for this system was determined as before. In several cases where the constants for the two series were in bad agreement the tests were repeated for both test antigens. In such cases the results of the new tests are recorded in the table with the old constants in parentheses.

Table V  
Inhibition by Simple Haptens

Hapten	Hapten concentration						$K_a$	$K_b$
	$10^{-6}$	$150 \times 10^{-6}$	$50 \times 10^{-6}$	$16.7 \times 10^{-6}$	$100 \times 10^{-6}$	$0.01 \text{ M}$		
1  (comp. III) a - - - - 100 100 98 7 b - - - - 100 100 100 5								
2  (comp. II) a - - - - 100 100 88 6.5 b - - - - 100 100 100 5								
3  a - - - 100 93 55 4.1 b - - - - - - - -								
4 p-NHCOCH <sub>3</sub> (benzoic acid) a - - - - 99 91 57 4.1 b - - - - 70 48 29 2.4								
5 Brown impurity from short dyes a - - - - 100 95 50 3.7 b - - - - 100 100 52 4.4								
6 p-NO <sub>2</sub> (benzoic acid) a - - - - 83 56 32 2.3 b - - - - 55 38 21 1.8								
7  a - - - 93 51 21 1.9 b - - - - 80 46 27 2.4								
8  a - - - - 84 46 23 1.8 b - - - - 67 42 20 2.1								

a % inhibition of precipitation by the simple test antigen.

b % inhibition of precipitation by the azo-ovalbumin test antigen.

$K_a$  Relative inhib. const. for precip. by the simple test antigen.

$K_b$  Relative inhib. const. for precip. by the azo-oval. test antigen.

Table V (cont.)

9	p-OCH <sub>3</sub> (benzoic acid)	-	-	-	73	41	24	1.7
		-	-	-	47	27	16	1.5
10	p-Br(benzoic acid)	-	-	-	55	23	15	1.0
		-	-	-	40	.22	8	1.3
11	p-Cl(benzoic acid)	-	-	-	50	27	15	1.0
		-	-	-	36	20	9	1.1
12	p-CH <sub>3</sub> (benzoic acid)	-	-	-	52	24	8	1.0
		-	-	-	35	23	14	1.1
13	p-COOH(benzoic acid)	-	-	-	47	25	9	1.0
		-	-	-	28	20	11	0.9
14	o-NH <sub>2</sub> (benzoic acid)	100	99	76	42	19	4	0.8
		-	-	-	35	25	15	1.1
15	p-OH(benzoic acid)	-	-	-	47	21	11	0.8
		-	-	-	26	14	13	0.9(0.6)
16	p-F(benzoic acid)	-	-	-	37	17	10	.7
		-	-	-	21	12	7	.6
17	m-COOH(benzoic acid)	-	-	-	37	16	10	.7(0.5)
		-	-	-	27	18	12	.9(.9)
18	 COOH	99	98	68	34	11	7	.6(.6)
		-	-	-	42	23	10	1.3(1.8)
19	p-NH <sub>2</sub> (benzoic acid)	99	87	45	25	16	10	.55
		-	-	-	18	8	6	.5
20	m-Cl(benzoic acid)	-	-	-	22	12	8	.45
		-	-	-	19	11	10	.6

Table V (cont.)

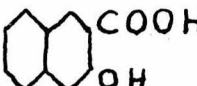
21	m-OH(benzoic acid)	-	-	-	18	13	9	.45
		-	-	-	14	8	5	.4
22	Benzoic acid	91	87	43	18	2	0	.4
		97	59	26	-	-	-	.4
23	2,4-di-OH(benzoic acid)	97	67	27	15	9	5	.31
		81	43	19	-	-	-	.3
24		96	72	17	10	4	2	.31 (.31)
		100	75	39	17	8	1	.5 (.5)
25	m-NH <sub>2</sub> (benzoic acid)	95	65	30	16	9	4	.31
		71	36	16	-	-	-	.25
26	m-I(benzoic acid)	92	51	17	15	7	3	.28
		100	60	27	-	-	-	.4
27	m-Br(benzoic acid)	-	-	-	14	9	3	.28
		100	63	35	-	-	-	.4
28	m-NHCOCH <sub>3</sub> (benzoic acid)	84	58	28	11	11	4	.28
		93	40	21	-	-	-	.3
29	o-OH(benzoic acid)	89	51	22	15	9	2	.28
		75	42	20	-	-	-	.3
30	m-CH <sub>3</sub> (benzoic acid)	77	47	22	16	9	3	.20
		92	48	25	-	-	-	.3
31	o-Cl(benzoic acid)	78	41	17	11	8	4	.20
		59	31	13	-	-	-	.22
32	m-NO <sub>2</sub> (benzoic acid)	66	38	15	5	0	0	.19
		75	40	18	-	-	-	.3

Table V (cont.)

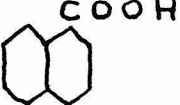
33	$\text{o-NHCOCH}_3$ (benzoic acid)	61 60	38 35	25 22	11 -	4 -	5 -	.19 .22
34	$\text{o-Br}$ (benzoic acid)	54 44	24 19	10 6	8 -	4 -	1 -	.16 .16
35	$2,4\text{-di-NO}_2$ (benzoic acid)	47 42	23 21	8 12	6 -	0 -	0 -	.14 .16
36	$\text{o-NHC}_6\text{H}_5$ (benzoic acid)	41 70	9 45	1 19	3 -	3 -	2 -	.12 .3
37	$\text{o-OCH}_3$ (benzoic acid)	30 40	17 23	10 16	10 -	10 -	7 -	.09 .16
38	$2\text{-OH, 3-NO}_2$ (benzoic acid)	33 31	11 54	7 14	4 -	2 -	1 -	.09 .11-.14
39	$\text{H}_2\text{N} \begin{array}{c} \text{C}_6\text{H}_4 \\ \text{---} \\ \text{N} \end{array} \text{N} \begin{array}{c} \text{C}_6\text{H}_4 \\ \text{---} \\ \text{AsO}_3\text{H}_2 \end{array}$	- -	15 8	5 5	- -	- -	- -	.09 0
40	$\text{o-CH}_3$ (benzoic acid)	30 50	14 24	3 13	5 -	4 -	3 -	.08 .16
41		16 55	9 34	8 20	3 -	4 -	2 -	.05 .22
42	$\text{o-NO}_2$ (benzoic acid)	10 19	2 11	0 7	0 -	2 -	-2 -	.03 .07
43	$\text{NaH}_2\text{PO}_4$	12 4	5 3	2 5	- -	- -	- -	.03 0
44	$2,4,6\text{-tri-NH}_3\text{Cl}$ (benzoic acid)	10 3	5 4	2 0	2 -	5 -	5 -	.03 0

Table V (cont.)

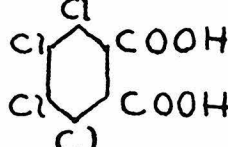
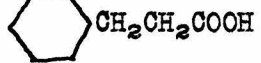
45	o-COOH(benzoic acid)	4 14	4 12	3 9	-2 -	-3 -	-1 -	0 .	.07
46	Na <sub>2</sub> SO <sub>4</sub>	5 7	3 8	2 4	-	-	-	0 0	
47	3,5-di-COOH(benzoic acid)	5 6	0 4	1 -2	-1 -	0 -	2 -	0 0	
48	HOOC  COOH	-3 8	4 3	7 3	8 -	5 -	3 -	0 0	
* 49	Phenylsulfonic acid	-5 9	-1 6	-1 4	3 -	2 -	5 -	0 0	
50	Phenylarsonic acid	4 7	3 5	1 5	-	-	-	0 0	
51	CH <sub>3</sub> COOH	-1 -	1 -	1 -	-	-	-	0 -	
52	CH <sub>3</sub> CH <sub>2</sub> COOH	0 -	2 -	3 -	-	-	-	0 -	
* 53	2,4,6-tri-NO <sub>2</sub> (benzoic acid)	1 36	-14 23	-9 12	-4 -	-2 -	1 -	-.05 .14	
* 54	Cyclohexanecarboxylic acid	-15 16	-1 6	0 3	-1 -	1 -	2 -	-.05 .07	
55	2,4,6-tri-CH <sub>3</sub> (benzoic acid)	-17 16	-7 11	-4 9	3 -	1 -	0 -	-.05 .07	
56	Cl  COOH	-12 18	-11 12	-7 8	-5 -	-1 -	-4 -	-.05 .07	

Table V (concl.)

57	3,5-di-NO <sub>2</sub> (benzoic acid)	-16 18	-13 10	-5 6	-3 -	1 -	-1 -	-.05 .07	
* 58		-26 12	-10 8	-4 7	-4 -	-3 -	-1 -	-.05 .04	
59		- -	-17 27	-6 11	- -	- -	- -	-.07 .22	
60	2-OH, 3,5-di-NO <sub>2</sub> (benzoic acid)	-29 37	-30 25	-12 17	-4 -	-3 -	-3 -	-.07 .16	
* 61		-20 20	-12 11	0 7	-3 -	-3 -	-2 -	-.07 .07	
62	o-COC <sub>6</sub> H <sub>5</sub> (benzoic acid)	-24 16	-14 10	-3 7	1 -	-1 -	1 -	-.07 .07	
63	2-OH, 5-NO <sub>2</sub> (benzoic acid)	24 57	-2 31	-6 10	-2 -	-3 -	2 -	?	.22

#### Discussion of Hapten Inhibition

A comparison of the inhibiting powers of the various haptens gives insight into the nature of the bonding of the haptens with the antibody molecules. In particular, comparisons of benzoic acid with various substituted benzoic acids is of great value. This comparison, discussed more fully below, indicates that substituents in the para position tend to increase the inhibiting power, whereas substituents in the meta or ortho positions decrease the inhibition.

The effect of substituents in the para position.--In every case studied, a substituent in the position para to the carboxy group increased the inhibition constant relative to the corresponding hapten without the para substituent (Tables VI and VII). In most cases the constant was increased by a factor of 1.1 to 2.5. Groups joined by N=N linkage (the link present in the immunizing antigen) were especially effective (compounds 1, 2, 3, 5, 7, and 8), suggesting that the complimentary structure of the antibody molecules involves the N=N group. Also p-NHCOCH<sub>3</sub>(benzoic acid) and p-NO<sub>2</sub>(benzoic acid) haptens (compounds 4, 6, and 33) were unusually good (Tables VI and VII), being 6 to 10 times as effective as corresponding benzoic acid derivatives without the group. This may be due to the presence of a double bonded oxygen capable of forming a hydrogen bond with -NH<sub>2</sub> or other groups on the antibody molecules.

The effect of meta substituents.--A single meta substituent slightly decreased or did not affect the inhibition in every case (Tables VI and VII). The exception, m-COOH(benzoic acid), which showed an increase, is discussed separately. The decrease was by a factor of 1 to 0.5. Substituents in both meta positions reduced the inhibition to zero or less (Tables VI and VII). The effect of meta substituents in preventing the hapten from combining with the antibody is probably steric.

The effect of ortho substituents.--Ortho substituents were more effective than the meta groups, generally reducing the inhibition constant by a factor of 0.8 to 0.2. The effect was probably steric

in this case also.  $\text{o-NO}_2$ (benzoic acid) and  $\text{o-COOH}$ (benzoic acid) gave practically no inhibition, possibly due to chelation which destroyed the resemblance to benzoic acid. A striking exception to the rule was furnished by  $\text{o-NH}_2$ (benzoic acid) which gave twice the inhibition of unsubstituted benzoic acid. All compounds with both ortho positions occupied had a negative inhibition constant. It seems likely that hapten inhibition studies might be useful in determining the structure of organic molecules, as for example deciding between a 3,4 and a 3,5 di-substituted benzoic acid.

Haptens with two carboxy groups in meta or para positions.-- Compounds with two carboxy groups can combine with the antibody in two ways and hence should be better inhibitors than benzoic acid. This was found to be true in cases where steric interference by other substituents would not be expected to prevent the combination (compounds 13 and 17).

Compounds with carboxy groups not attached to a benzene ring.-- One might expect that the presence in a hapten of an isolated carboxy group would give rise to fairly good inhibition. In no case was this found to be true (see compounds 51, 52, 54, 58, and 61).

Discrepancies among the inhibition constants.--For the most part, the constants for inhibition of precipitation by the simple test antigen and by the azo-ovalbumin test antigen are about the same. In several cases however there was a distinct difference. Furthermore the values of the inhibition constants at different hapten concentrations were not always in exact agreement. Both these discrepancies are probably related to the heterogeneity of the anti-serum which may contain antibody molecules differing in the extent to which they are complementary to the antigen and hapten molecules.

Haptens giving increased precipitation.--Several haptens markedly increased the amount of precipitate obtained compared with the amount that could be obtained with any concentration of the simple test antigen in the absence of added hapten. All the haptens which showed this phenomenon were ones in which some interaction

Table VI

Relative Inhibition Constants for Mono-substituted Benzoic Acid

substituents		para	meta	ortho
-NHCOCH <sub>3</sub>	$K_a$	4.1	2.8	0.19
	$K_b$	2.4	0.3	0.22
-NO <sub>2</sub>		2.3	0.19	0.03
		1.8	0.3	0.07
-OCH <sub>3</sub>		1.7	-	0.09
		1.5	-	0.16
-Cl		1.0	0.45	0.20
		1.1	0.6	0.22
-Br		1.0	0.28	0.16
		1.3	0.4	0.16
-I		-	0.28	0.2
		-	0.4	0.2
-CH <sub>3</sub>		1.0	0.20	0.08
		1.1	0.3	0.16
-COOH		1.0	0.7	0
		0.9	0.9	0.07
-OH		0.8	0.45	0.28
		0.9	0.4	0.3
-F		0.7	-	-
		0.6	-	-
-NH <sub>2</sub>		0.55	0.31	0.8
		0.5	0.25	1.1
-NHCO <sub>2</sub> H <sub>5</sub>		-	-	0.12
		-	-	0.3
-COOC <sub>6</sub> H <sub>5</sub>		-	-	-0.07
		-	-	0.07
unsubstituted benzoic acid		4	4	4

$K_a$  Relative inhib. const. for precip. by the simple test antigen.

$K_b$  Relative inhib. const. for precip. by the azo-oval. test antigen.

Table VII  
Inhibition Constants for Poly-substituted Benzoic Acid

Effect of para substituents		Effect of ortho substituents	
2,4-di-OH	$K_a$ $K_b$	0.8 0.9	 $K_a$ $K_b$
o-OH		0.28 0.3	 $K_a$ $K_b$
---			 $K_a$ $K_b$
2,4-di-NO <sub>2</sub>		0.14 0.16	0.05 0.22
o-NO <sub>2</sub>		0.03 0.07	2-OH, 3-NO <sub>2</sub> m-NO <sub>2</sub>
---			0.09 0.11 0.19 0.3
Effect of meta substituents		2,4-di-NO <sub>2</sub>	
2-OH, 3-NO <sub>2</sub>	$K_a$ $K_b$	0.09 0.11 (.4)	4-NO <sub>2</sub>
o-OH		0.45 0.4	2-OH, 3,5-di-NO <sub>2</sub>
---			-0.07 0.16
3,5-di-NO <sub>2</sub>		-0.05 0.07	3,5-di-NO <sub>2</sub>
m-NO <sub>2</sub>		0.19 0.3	2,4,6-tri-NO <sub>2</sub>
---			-0.05 0.14
3,5-di-COOH		0 0	2,4-di-NO <sub>2</sub>
benzoic acid		0.4 0.4	p-NO <sub>2</sub>
---			0.14 0.16
2-OH, 3,5-di-NO <sub>2</sub>		-0.07 0.07	2,4,6-tri-NH <sub>3</sub> Cl
o-OH		0.28 0.3	2,4,6-tri-CH <sub>3</sub>
---			p-CH <sub>3</sub>
			1.0 1.1

$K_a$  Relative inhib. const. for precip. by the simple test antigen.

$K_b$  Relative inhib. const. for precip. by the azo-oval. test antigen.

with the antibody molecules would be expected, but where the reaction would be extremely weak. It was suggested that strong haptens in very dilute concentrations might also give an increase. However if this were true one would also expect moderately weak haptens to give an increase in moderately dilute concentrations. This was not observed. It is possible that the antiserum contains much very low grade monovalent antibody which combines with the carboxy group but does not closely fit the benzene ring. This antibody could form soluble complexes with the simple test antigen, with a resultant decrease in the amount of precipitate. A hapten added to the solution would combine with this low grade antibody tending to increase the amount of precipitate. However, only haptens with large substituents in ortho and meta positions or with an isolated carboxy group would react preferentially with the low grade antibody leaving the strong antibodies free to combine with the test antigen.

Conclusion.--These experiments apparently show that many of the antibody molecules fit the benzoic acid groups rather closely and form bonds with suitable constituents in the para position. The fact that ortho and meta substituted haptens do show considerable inhibition may mean that such haptens combine under some strain with the antibody or it may mean that there are some antibody molecules present which fit loosely around the benzene ring.

References

1. K. Landsteiner and J. van der Scheer, J. Exptl., 63, 325 (1936)
2. K. Landsteiner and J. van der Scheer, Proc. Soc. Exptl. Biol. Med., 29, 747 (1932)
3. L. Pauling, D. Pressman, D. H. Campbell, C. Ikeda, and M. Ikawa, J. Am. Chem. Soc., 64, 2994 (1942)
4. L. Pauling, J. Am. Chem. Soc., 62, 2643 (1940)
5. K. Lansteiner and J. van der Scheer, J. Exptl. Med., 55, 781 (1932)
6. F. G. Pope and W. I. Willett, J. Chem. Soc., 1259 (1913)  
H. Bucherer and A. Schwalbe, Ber., 39, 2798 (1906)
7. O. Folin and V. Ciocalteu, J. Biol. Chem., 73, 627 (1927)
8. D. Pressman, D. H. Brown, and L. Pauling, J. Am. Chem. Soc., 64, 3015 (1942)
9. L. Pauling, D. Pressman, D. H. Campbell, and C. Ikeda, J. Am. Chem. Soc., 64, 3003 (1942)
10. S. B. Hooker and W. C. Boyd, Proc. Third Internat. Cong. Microbiol., p. 814 (1940)
11. K. Landsteiner and J. van der Scheer, J. Exptl. Med., 48, 315 (1928); 50, 407 (1929); 54, 295 (1931)
12. K. Landsteiner, Biochem. Z., 93, 117 (1919); 104, 280 (1920)

Part III

The Construction and Operation of a Tiselius  
Electrophoresis Apparatus

Part III  
The Construction and Operation of a Tiselius'  
Electrophoresis Apparatus

The electrophoretic motion of colloidal particles has been studied intermittently for over a century. The nature of the substances studied has been determined largely by the technics that have been developed. Thus early work was done with clays, individual particles of which could be seen microscopically. Later, studies were made on sub-microscopic particles with the aid of the ultra microscope. Recently methods have been developed for observing the motion of the entire mass of a solution of a substance under investigation rather than individual particles. The usual procedure is to put the solution to be studied in the bottom of a U tube and layer over it another solution of lower density. On passing an electric current through the U tube, the boundary between the layers will move with the velocity of the particles in the lower layer. The position of the boundary may be noted by the color of the solution or by ultra violet absorption in favorable cases.

The Toepler schlieren optical method for observing a boundary was applied to electrophoresis by Tiselius (1) in 1937. This technic, with improvements by Longsworth and MacInnes (2) and others, has made the analysis and purification by electrophoresis of proteins and other colorless solutions an important branch of modern science. In this thesis I am presenting a description of a Tiselius' electrophoresis apparatus built at the California Institute during 1942-1943. The apparatus is based on Longsworth's design and incorporates certain improvements which are discussed.

The Foucault-Toepler schlieren optical system.--Light passing through the diffuse boundary between two solutions in a U tube will be refracted downward due to the vertical gradient of the refractive index of the solution within the boundary region. The schlieren optical system, illustrated in figure 1, is designed to intercept all the refracted light so that the boundaries appear black. In this system the camera lens throws an image of the cell

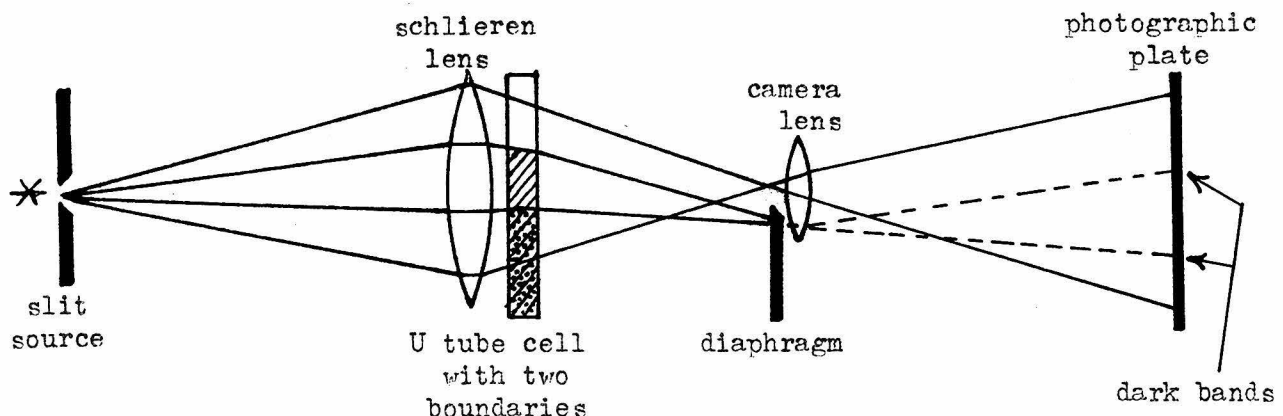
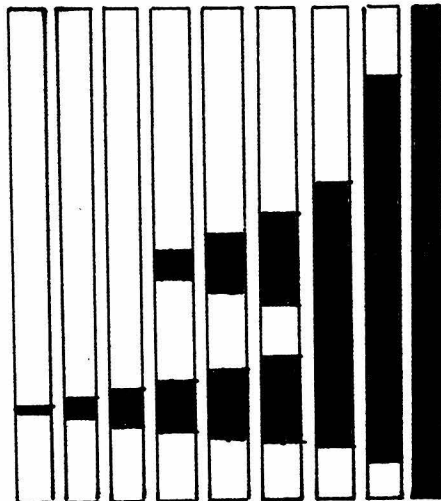
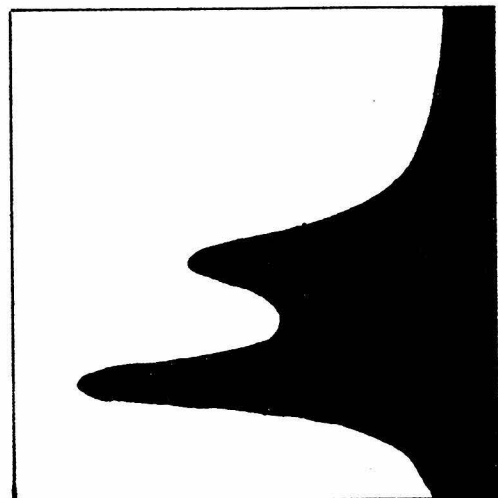


Figure 1  
(side view)

on the photographic plate. Instead of illuminating the cell with diffuse light as in ordinary photography, the schlieren system has a large lens (the schlieren lens) just in front of the cell and a distant slit source of light arranged so that all unrefracted rays of light converge at a point just in front of the camera lens. Rays refracted downward by the boundaries are intercepted by an opaque diaphragm with a straight horizontal edge immediately below the point of convergence. Hence the image of the cell on the photographic plate will be crossed by black bands at the positions of boundaries in the cell. With a good optical system the method is extremely sensitive. Furthermore it is possible to measure the height of the diaphragm or take a series of pictures with different diaphragm settings (fig. 2), and thus get a quantitative measure of the refractive index gradient in all parts of the cell. Longsworth introduced a mechanical system for steadily raising the diaphragm while the photographic plate moves sideways over the cell image, thus getting a continuous pattern of the boundaries. He used a



A series of schlieren photographs



Continuous schlieren scanning

Figure 2

long vertical slit in front of the photographic plate to mask out all but a narrow portion of the cell. This continuous scanning system is the basis of our apparatus.

Since the refractive index gradient is proportional to the protein concentration gradient, the area of a peak on the pattern is proportional to the increment of protein concentration between the layers forming the boundary. The combination of electrophoresis and schlieren-scanning is thus a quantitative as well as a qualitative analytical tool.

The use of parabolic mirrors.--In place of the usual schlieren lens and camera lens we used two parabolic mirrors, 6 inches and 8 inches in diameter, and two small flat diagonal mirrors. The mirrors are aluminized glass with focal lengths 48 inches and 60 inches respectively. The optical arrangement is illustrated in figure 3. The slit system, on the optical axis of the mirrors, is illuminated, with the aid of a small diagonal mirror, by a source and condenser lens placed to one side. Light from the slit falls on the 6" mirror and is sent back parallel through the cell and to the 8" mirror at the other end of the apparatus. The 8" mirror serves the combined function of converging the light at the position of the diaphragm and of forming an image of the cell on

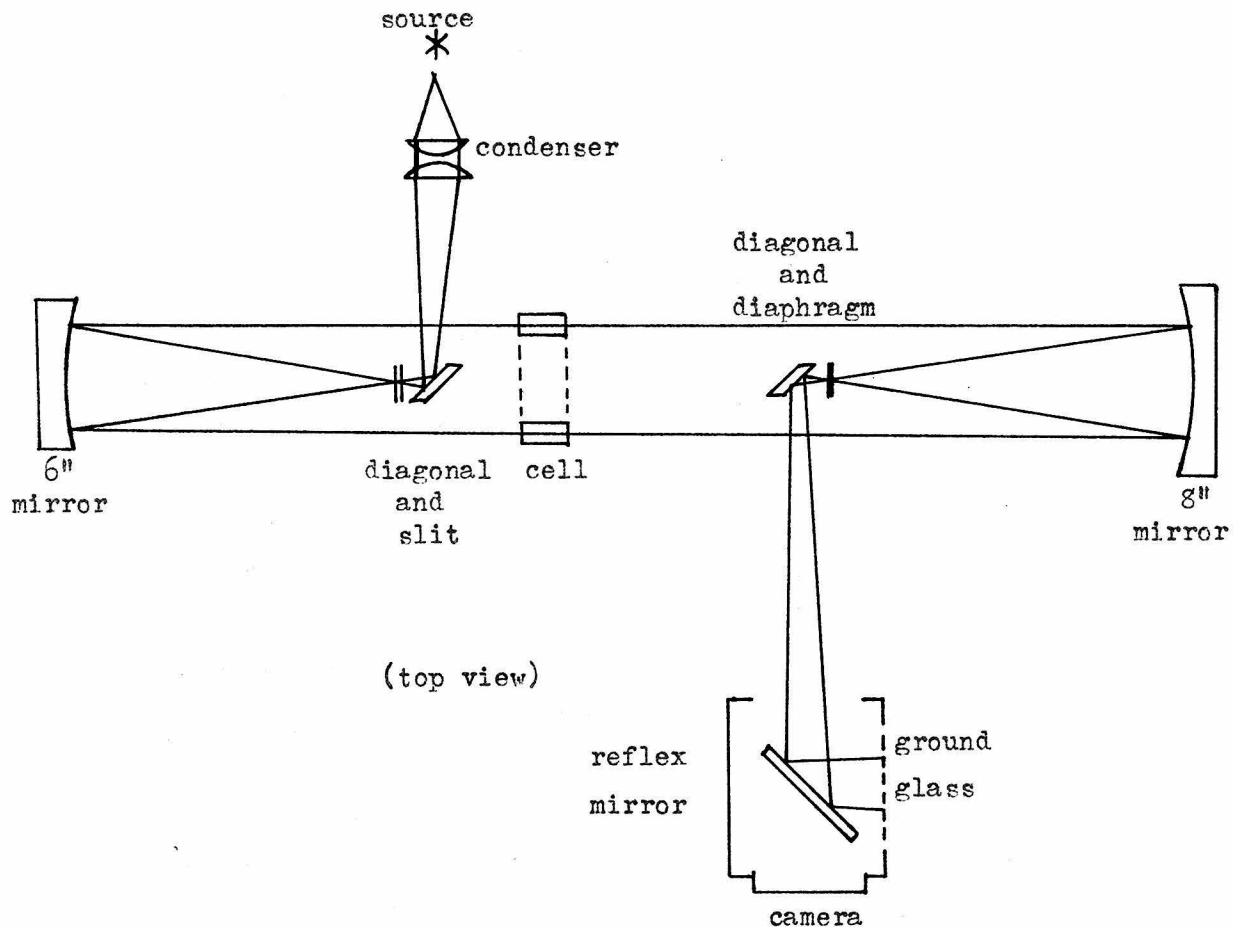


Figure 3

the photographic plate, thus eliminating the need of a camera lens. The optical parts cost about \$80 and have proved to be excellent. An equivalent lens system would require a 5 inch achromatic schlieren lens of excellent definition and a 2 inch achromatic camera lens of fair quality. The cost of the lenses would be about \$400 to \$600. At the time the apparatus was built suitable lenses were not available. An added advantage of the mirrors is that they are completely achromatic so that they can be used with infra red light for studying certain highly colored solutions.

A disadvantage of the system is that the slit and diaphragm are in the optical path and cast a shadow an inch wide and the full height of the field of view. This does no harm if the limbs of the U tube cell are far enough apart to straddle the shadow.

Mounting the optical parts.--The mirrors are supported on mounts that permit rotation about vertical and horizontal axes by means of tangent screws. In this respect lenses have the advantage of requiring less elaborate mountings. The tangent screw for rotating the small diagonal mirror has a long shaft connected by flexible couplings and terminating in a knob at the camera. This permits an operator to center the cell image on the long vertical slit in front of the photographic plate. The main optical bench was made from two 16 ft. lengths of 6 inch channel iron held 4 inches apart by several plates welded in place. A single I beam would probably be satisfactory and cheaper. This beam, supported at two points by cement blocks, carries all the parts except the camera. A third cement block supports the camera.

The camera and reflex mirror.--The camera design incorporates a pivoted mirror which can be swung into a diagonal position to throw the cell image on a ground glass plate at the side of the camera. This permits visual inspection of the electrophoretic pattern without removing the plate holder and vertical slit. 5" x 7" plates are used, permitting unusually long electrophoretic patterns to be photographed. To conserve photographic plates and to get a series of exposures on one plate, either half of the plate can be masked by a sector built into the camera. Vertical reference lines can be left on the plates by flashing a small light in the tube of the camera. This exposes the plate through the slit.

Light source.--A simple ribbon filament lamp drawing 18 amperes at 6 V is used as the source instead of the mercury vapor arc frequently employed. A non-achromatic condenser lens and a total reflecting prism focus the light on the slit. Good optical parts are not necessary here. Color filters placed over the condenser lens are used when colored solutions are being examined.

Scanning mechanism.--A frame carrying the plate holder is moved horizontally by a screw turned by a Bodine synchronous motor, 1/2 R.P.M. The frame rolls smoothly on a track instead of sliding as in Longsworth's design. A shaft leading to the diaphragm mechanism is coupled with the camera screw shaft by a pair of spur gears and a pair of spiral gears which reduce the speed 1/3. The spur gears are interchangeable for varying the relative velocity of the diaphragm and plate. This is essentially Longsworth's arrangement. A friction clutch disconnects the diaphragm shaft so that it can be turned by hand. The position of the diaphragm can be read on a revolution counter connected to the shaft. The diaphragm is raised by another screw coupled with the shaft by bevel gears. The motor may be disconnected from the system by disengaging a multi-jaw coupling. Limit switches were installed on both screws for protection.

Control of temperature.--To minimize convection currents arising in the cell from heat generated by the passage of the current, the electrophoresis must be done in a cold bath at a temperature near that of maximum density of the solution. The optimum temperature is discussed later in greater detail.

The tank in our apparatus is made of galvanized iron in a welded angle iron frame. It is insulated with 2 inches of tarred celotex. A refrigerator runs continuously to cool the thermostat at a constant rate. A specially designed expansion valve, made according to the plans of Roper (3), limits the flow of refrigerant to slightly more than is necessary to keep the bath cold. A motor, mounted on an independent bracket on the wall, stirs the bath vigorously. A mercury filled thermoregulator controls an intermittent electric heater which maintains the desired temperature to  $\pm 0.03^\circ$ .

There are windows made of ground and polished plate glass in opposite sides of the bath. These windows are double, with a dry air space between, to reduce the condensation of water on the cold glass. The windows are pivoted, one about a horizontal axis and

one about a vertical axis, the connection with the tank being made by a soft rubber disc. This arrangement permits the windows to be set exactly parallel to eliminate the chromatic aberrations that would result otherwise. Furthermore, by tilting one window, the refraction caused by very sharp boundaries can be partially compensated, bringing the boundary within the range of the apparatus, and partially correcting the chromatic aberration of the boundary. Probably this feature is an unnecessary refinement, and adequate care in building the windows in good alignment would suffice.

One window projects into the tank to reduce the length of the light path in the water. This is also not essential.

Cells.--Electrophoresis cells were made in three sections according to the design of Tiselius as improved by Longsworth. The top section joins the cell to the two electrode vessels. The middle section consists of the two limbs of the U tube. The limbs are made of 1/8 inch optical quality plate glass cemented together to form rectangular tubes 1/8 by 1 inch. The bottom section merely joins the two limbs. Between the sections are pairs of horizontal glass plates which can slide over each other. The parts of each section are cemented to these plates. There are rectangular holes in the plates making the assembled cell a continuous U tube. This sliding sectional arrangement permits one to fill the cell with layers of solution and form sharp boundaries between them.

None of the usual laboratory cements proved satisfactory for making the cells. We finally found a formula (4) for a high temperature cement that gives very good joints though it is difficult to use. This cement is really a low melting glass. The ingredients

calcined borax	4 parts
red lead	16 parts
washed silicic acid	5 parts

are finely ground and intimately mixed. The mixture is then fused in a crucible with a blast lamp until homogeneous and finally poured out to cool. Thorough premixing saves time during the melting. We found it best to powder the cement to a flour and

mix it to a smooth paste with water. If it is sufficiently fine it may be flowed evenly, with a small brush, onto the edges to be joined. Even application is essential. After the paste dries it is still quite adherent and the high spots can be rubbed off on a ground glass plate. The glass parts are assembled and the cement fused in a muffle furnace for 1 to 3 hours at just below the softening point of the glass. The best temperature was one that imparted a slight glow to the furnace, perceptible only in a darkened room. Moderate pressure helps to form good joints. We found it best to fuse the tubes of the center section first and then cement them to the sliding plates. In this way we were able to make good cells practically free from optical distortion. The cement worked well for pyrex to pyrex, or to join several different brands of plate and window glass. Joints between plate glass and soft glass tubing frequently developed many fine cracks. All the joints were very strong but were quite sensitive to shock.

Improved cell holders.--A suitable cell holder must slide the sections back and forth without straining the glass. In our apparatus the top section is held in one position, though it is free to tilt so that strains cannot be set up. A rack and pinion arrangement on the holder moves a frame which carries both the middle and lower sections, sliding them past the upper section. The force necessary to slide the plates is applied directly on the edge of the plate so that the cell is not strained. A second rack and pinion mounted on this moving frame slides the lower section past the middle section. In supporting the cell, over-constraint has been avoided and no twisting or bending strain can be put on the glass. The frame is easily adjusted to fit several sizes of cell.

Arrangement for running two experiments at once.--Both the electrode vessels are mounted in the cell holder on the same side of the cell. Two identical units were built so that they can be put in the thermostat tank with the cells adjacent. This permits two runs to be made at once. The cell holders roll on tracks across the top of the tank so that either cell can be put in the

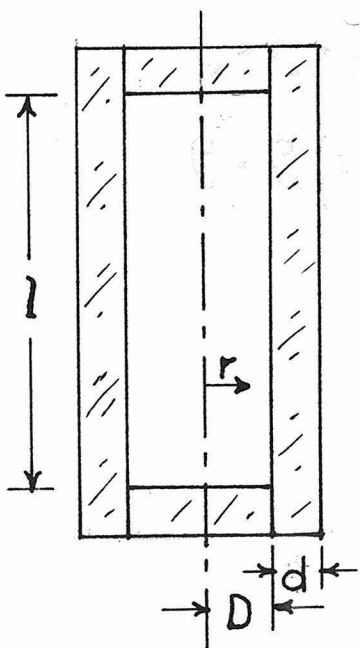
optical path. As yet this idea has not been tried.

Power supply and current control.--A rectifier with current regulating tubes supplies the power. The current is measured with a fixed resistance and potentiometer. Currents of 10 to 20 milliamperes are generally used.

### The Optimum Temperature for Electrophoresis

As mentioned earlier, the current passing through the cell will generate heat which will be dissipated only at the walls of the cell. For this reason the center of the cell will be warmer than the walls and convection currents may be set up. The temperature differences in the cell are determined only by the current and by the thermal and electrical conductivity of the solution. Of these, only the current can be varied in ordinary electrophoretic work. For the sake of economy of time it is desirable to have the current as high as possible. Fortunately, by working near the temperature of maximum density of the solution, the density differences for given temperature differences can be greatly reduced. Most work has been done at a bath temperature of  $1.5^{\circ}$  to  $3^{\circ}$  C. without any exact knowledge as to the optimum temperature. It is obvious that convection can be reduced still more by adjusting the temperature so that the solution has its maximum density within the cell at a point about half way between the center and the edge. A derivation of the density distribution and the optimum temperature follows.

Derivation of temperature distribution.--In this derivation it will be assumed that all the heat is conducted perpendicular to a plane through the center of the cell and that none is conducted through this plane.



$i$  = current density

$I$  = total current through cell

$L$  = specific conductivity of solution

$T_c$  = temperature at center of cell

$T_r$  = temperature as function of  $r$

$T_w$  = temperature at inside wall

$T_o$  = temperature at outside wall

$\lambda_s$  = heat conductivity of solution

$\lambda_g$  = heat conductivity of glass

Let  $q' = -\frac{dT}{dr} \lambda_s$  be the rate of heat transfer through a unit area parallel to the central plane.  $q'$  must also equal the rate at which heat is generated between the unit area and the central plane.

$$\therefore -\frac{dT}{dr} \lambda_s = \frac{i^2 r}{L}$$

Integrating and applying boundary conditions,

$$T_r = T_w + \frac{i^2}{2\lambda_s L} (D^2 - r^2) \quad (1)$$

Similarly, for the heat transfer through the glass walls,

$$T_w = T_o + \frac{i^2 dD}{\lambda_g L} \quad (2)$$

Derivation of density distribution. --To get the corresponding density distribution in the cell it is convenient to refer the densities to the maximum value,  $\rho_m$ , and refer temperatures to the temperature of maximum density,  $T_m$ . The density of a solution as a function of the temperature can be approximated by the quadratic equation,

$$\rho_r = \rho_m \left\{ 1 - a(T_r - T_m)^2 \right\} \quad \text{where } a \text{ is a constant of the solution whose value need not be known.}$$

Substituting  $T_r$  from equation (1),

$$\rho_r = \rho_m \left\{ 1 - a \left[ T_w - T_m + \frac{i^2}{2\lambda_s L} (D^2 - r^2) \right]^2 \right\} \quad (3)$$

Let  $r_m = nD$  be the value of  $r$  at the point within the cell where the density is a maximum. Then

$$T_w - T_m + \frac{i^2}{2\lambda_s L} (D^2 - r_m^2) = 0 \quad \text{giving}$$

$$\rho_r = \rho_m \left\{ 1 - \frac{ai^4 D^4}{4\lambda_s^2 L^2} \left( n^2 - \frac{r^2}{D^2} \right)^2 \right\} \quad (4)$$

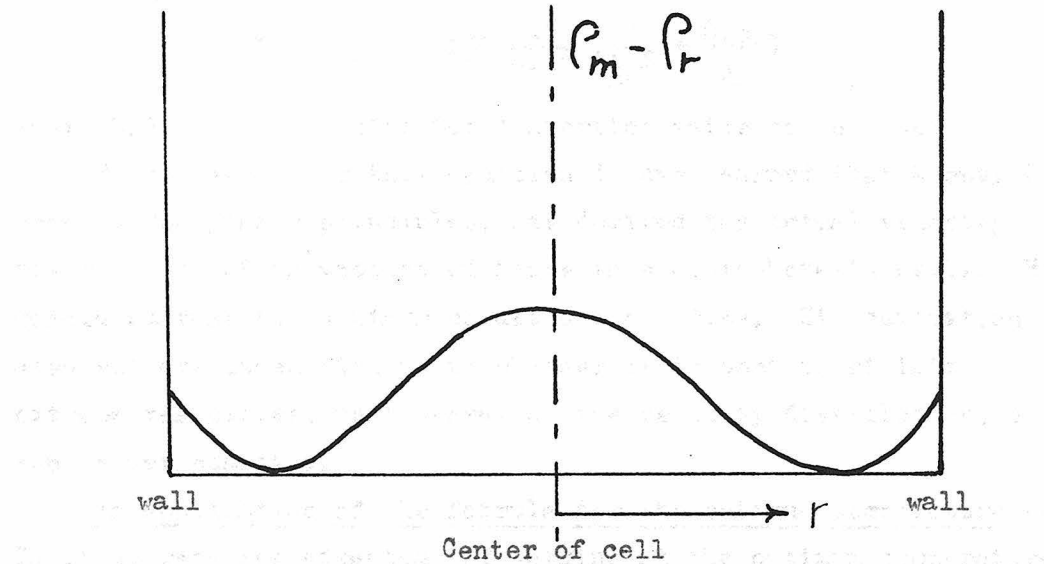
2. Derivation of equations of state for the cell can be accomplished by defining the following variables:

$$T = T_w - T_m + \frac{i^2}{2\lambda_s L} (D^2 - r^2)$$

It is now possible to express the state of the cell in terms of  $T$  and  $r$ .

For  $n = 0.8$  as an example, a graph of equation (4) will have the form,

graph of  $\rho_m - \rho_r$  vs  $r$  for  $n = 0.8$



It is not clear what value of  $n$  is best. The following two possibilities are presented.

1. Minimizing the area.--The area is given by

$$A \propto \int_0^D \left( n^2 - \frac{r^2}{D^2} \right)^2 dr = \left( n^4 D - \frac{2n^2 D}{3} + \frac{D}{5} \right)$$

Minimizing with respect to  $n$

$$\frac{dA}{dn} = 0 = 4n^3 D - \frac{4nD}{3} \quad \text{giving} \quad n = (1/3)^{1/2} = 0.58$$

2. Minimizing the greatest density difference will be accomplished by letting  $\rho_0 = \rho_D$  giving

$$n = (1/2)^{1/2} = 0.71$$

It seems probable that either of these two values or an intermediate value would be satisfactory. I am inclined to think that minimizing the area is the best procedure. Substituting  $n = 0.58$

in equations (1) and (2) and letting  $I = 2Dli$  gives the optimum bath temperature in the final form,

$$T_o = T_m - 0.239 \frac{I^2}{4Ll^2} \left( \frac{d}{\lambda_g^D} + \frac{0.33}{\lambda_s} \right) \quad (5)$$

where 0.239 is the factor for converting watts to cal./sec.

Since developing this equation I have learned that Mooney (5), using hydrodynamic principles, has derived the actual velocity distribution of convection currents in electrophoresis cells. He concludes that for optimum conditions  $n = 0.54$ . His derivation also suffers indecision as to whether it is best to minimize extreme velocities, an integral of the velocity distribution, or some other quantity.

An application of the formula for the optimum temperature.-- To illustrate the advantage of working at the optimum temperature, consider a typical electrophoresis experiment in a phosphate buffer solution.

$$L = 0.0038 \text{ ohm}^{-1} \text{cm.}^{-1}$$

$$T = 2.45^\circ\text{C.}$$

$$\lambda_s^m = 1.29 \times 10^{-3} \text{ cal./cm. sec. degree C.}$$

$$\lambda_g = 1.7 \times 10^{-3} \text{ cal./cm. sec. degree C.}$$

$$D = 0.198 \text{ cm.}$$

$$d = 0.317 \text{ cm.}$$

$$l = 2.5 \text{ cm.}$$

$$I = 0.020 \text{ amp.}$$

Substituting these values in equation (5) gives,

$$T_o = 2.45^\circ - 1.20^\circ = 1.25^\circ \text{ C.}$$

As an illustration of the advantages of working at the optimum temperature, fig. 4 shows the density differences in a cell in a bath at the optimum temperature, the temperature of maximum density, and at room temperature. The values of the current in the three cases are 20 ma., 10 ma., and 3.7 ma. respectively. These currents are about the maximum that can be used at the three temperatures. Thus by working at the optimum temperature one can reduce the time of an electrophoresis experiment by at least one-half.

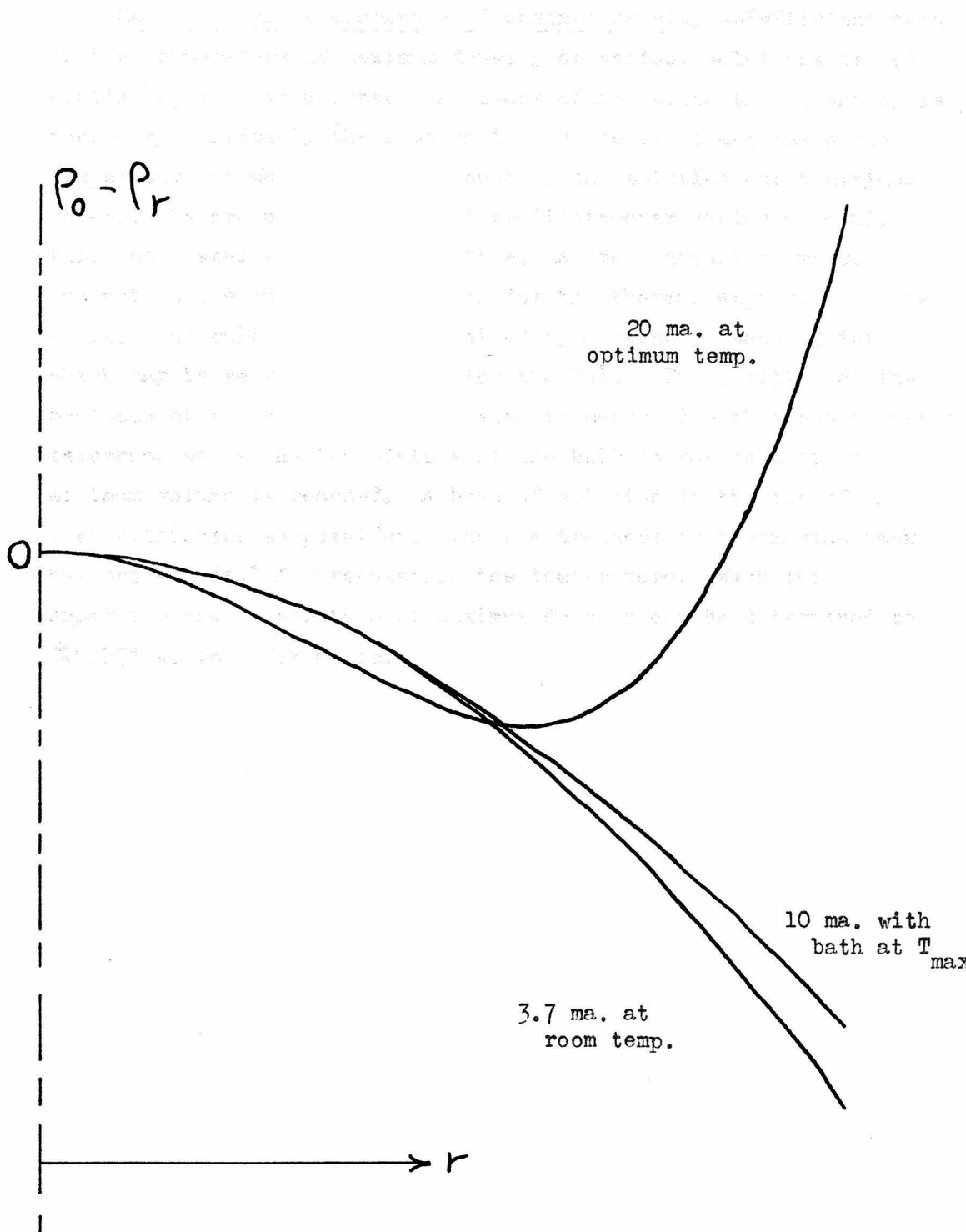


Figure 4

Measuring the temperature of maximum density.--Sufficient data on the temperature of maximum density of various solutions is not available, so that a convenient means of measuring this quantity is necessary. Probably the most rapid technic is to determine the temperature at which a given amount of the solution has a minimum volume. We are using a pyrex glass dilatometer having a 50 ml. bulb and a stem with a 1/2 mm. bore. A small amount of mercury was put in the bulb to compensate for the thermal expansion of the glass. The bulb and stem are joined by a standard taper joint which may be separated for filling the bulb. The position of the meniscus of the solution in the stem is measured with a cathetometer telescope while the temperature of the bulb is varied until a minimum volume is reached. A bead of solution in the top of the stem eliminates evaporation. The electrophoresis thermostat tank has proved ideal for regulating the temperature. With this apparatus the temperature of maximum density can be determined to  $\pm 0.05^{\circ}$  C. in a few hours.

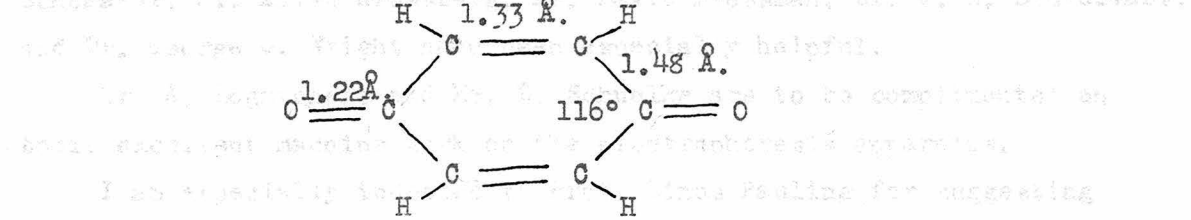
References

1. A. Tiselius, Trans. Far. Soc., 33, 524 (1937)
2. L. G. Longsworth and D. A. MacInnes, Chem. Rev., 24, 271 (1939)
3. E. Roper, Ind. and Eng. Chem., Anal. Ed., 13, 257 (1941)
4. Ernst von Angerer, Technische Kunstgriffe bei Physikalischen Untersuchungen, pub. by Friedr. Vieweg und Sohn, Braunschweig (1936)
5. M. Mooney, Temperature: Its Measurement and Control in Science and Industry, p. 428, pub. by American Institute of Physics.

Summary

The structures of  $SbI_3$ ,  $SbBr_3$ ,  $SbCl_3$ ,  $AsI_3$ ,  $AsBr_3$ ,  $AsCl_3$ ,  $PI_3$ ,  $PBr_3$ , and  $PCl_3$  in the gaseous state have been determined by electron diffraction. The results, page 27, show small but significant deviations from the Pauling-Huggins and Schomaker-Stevenson additivity rules. A serious discrepancy in electron diffraction data has been discussed.

Quinone in the vapor state has been found to have the structure,



Reactions between antibodies and benzoic acid derivatives have been studied qualitatively and quantitatively. The results indicate that the bonding involves complementary configurations of moderately close fit. Many factors are apparently involved in the reactions.

A Tiselius electrophoresis apparatus using parabolic mirrors has been described. An equation giving the optimum temperature for electrophoresis has been derived.

Introduction

Methodology

The following sections are to be read in conjunction with the text of the thesis.

Appendix A, B, C, D, E, F, G, H, I, J, K, L, M, N, O, P, Q, R, S, T, U, V, W, X, Y, Z.

Acknowledgement

Appendix

Parts of this thesis were done in collaboration with other workers, for whose assistance I am grateful. Dr. D. P. Stevenson, Dr. Verner Schomaker, Mr. Allen Grossberg, Dr. David Pressman, Dr. J. H. Sturdivant, and Dr. George G. Wright have been especially helpful.

Mr. A. Logatcheff and Mr. B. Schuelke are to be complimented on their excellent machine work on the electrophoresis apparatus.

I am especially indebted to Prof. Linus Pauling for suggesting and encouraging the work on these problems.

Appendix A, B, C, D, E, F, G, H, I, J, K, L, M, N, O, P, Q, R, S, T, U, V, W, X, Y, Z.

Appendix A, B, C, D, E, F, G, H, I, J, K, L, M, N, O, P, Q, R, S, T, U, V, W, X, Y, Z.

Appendix A, B, C, D, E, F, G, H, I, J, K, L, M, N, O, P, Q, R, S, T, U, V, W, X, Y, Z.

Appendix A, B, C, D, E, F, G, H, I, J, K, L, M, N, O, P, Q, R, S, T, U, V, W, X, Y, Z.

Appendix A, B, C, D, E, F, G, H, I, J, K, L, M, N, O, P, Q, R, S, T, U, V, W, X, Y, Z.

Appendix A, B, C, D, E, F, G, H, I, J, K, L, M, N, O, P, Q, R, S, T, U, V, W, X, Y, Z.

Appendix A, B, C, D, E, F, G, H, I, J, K, L, M, N, O, P, Q, R, S, T, U, V, W, X, Y, Z.

Appendix A, B, C, D, E, F, G, H, I, J, K, L, M, N, O, P, Q, R, S, T, U, V, W, X, Y, Z.

Appendix A, B, C, D, E, F, G, H, I, J, K, L, M, N, O, P, Q, R, S, T, U, V, W, X, Y, Z.

Appendix A, B, C, D, E, F, G, H, I, J, K, L, M, N, O, P, Q, R, S, T, U, V, W, X, Y, Z.

Appendix A, B, C, D, E, F, G, H, I, J, K, L, M, N, O, P, Q, R, S, T, U, V, W, X, Y, Z.

Appendix A, B, C, D, E, F, G, H, I, J, K, L, M, N, O, P, Q, R, S, T, U, V, W, X, Y, Z.

Appendix A, B, C, D, E, F, G, H, I, J, K, L, M, N, O, P, Q, R, S, T, U, V, W, X, Y, Z.

Appendix A, B, C, D, E, F, G, H, I, J, K, L, M, N, O, P, Q, R, S, T, U, V, W, X, Y, Z.

Appendix A, B, C, D, E, F, G, H, I, J, K, L, M, N, O, P, Q, R, S, T, U, V, W, X, Y, Z.

Appendix A, B, C, D, E, F, G, H, I, J, K, L, M, N, O, P, Q, R, S, T, U, V, W, X, Y, Z.

Appendix A, B, C, D, E, F, G, H, I, J, K, L, M, N, O, P, Q, R, S, T, U, V, W, X, Y, Z.

Appendix A, B, C, D, E, F, G, H, I, J, K, L, M, N, O, P, Q, R, S, T, U, V, W, X, Y, Z.

Appendix A, B, C, D, E, F, G, H, I, J, K, L, M, N, O, P, Q, R, S, T, U, V, W, X, Y, Z.

Appendix A, B, C, D, E, F, G, H, I, J, K, L, M, N, O, P, Q, R, S, T, U, V, W, X, Y, Z.

Appendix A, B, C, D, E, F, G, H, I, J, K, L, M, N, O, P, Q, R, S, T, U, V, W, X, Y, Z.

Appendix A, B, C, D, E, F, G, H, I, J, K, L, M, N, O, P, Q, R, S, T, U, V, W, X, Y, Z.

Propositions

1. Robertson's comparison of the C = O distance of 1.14 Å. which he found for quinone with the C = O distance of 1.16 Å. in carbon dioxide is illogical. Quinone should be compared with conjugated ketones.

Reference:

J. M. Robertson, Proc. Roy. Soc., 150, 106 (1935)

2. Contrary to statements made in seminar, the usual analysis of an electron diffraction radial distribution integral cannot in general give the structure of a molecule as accurately as the correlation of theoretical intensity curves.

3. Four minor improvements in the techniques of electron diffraction and x-ray diffraction are proposed.

a. The maxima and minima of electron diffraction photographs are the points where the gradient of density equals the estimated gradient of background density. This is one of the easiest and best ways of interpreting the photographs.

b. A method of separating two or more packets of I. B. M. cards after they have been summed but before they are resorted is proposed. The method involves the use of special index cards rather than separate files of cards.

c. A method of easily and rapidly making artificial electron diffraction photographs of any compound is suggested.

d. A special pair of calipers useful in indexing x-ray rotation photographs has been designed.

4. A good Tiselius electrophoresis apparatus using a 5" spherical mirror and two inexpensive non-achromatic lenses could be built for less than \$500. The proposed apparatus would be exceptionally compact and would give results comparable or superior to those obtained with most existing apparatuses.

5. It has been found that one of the most serious limitations of the Foucault-Toepler schlieren optical system, as applied to electrophoresis, is the diffuseness and poor resolution of the boundary pattern resulting from diffraction at the edge of the diaphragm. The complexity of the refraction in the boundaries apparently makes an analysis of the diffraction pattern difficult. I propose that:

- a. The diffraction may be treated satisfactorily as a case of a straight edge in a convergent or divergent cylindrical wave front.
- b. The simple optical system in proposition (4) would reduce the diffraction effects.

6. The electrophoresis apparatus has an excellent optical system which could be used advantageously in the following studies:

- a. Diffusion.
- b. Chromatography of colorless solutions. A small wedge shape cell at the outlet of the chromatograph column would enable one to measure continuously the refractive index of the emergent solution.
- c. The electrophoretic-diffusion equilibrium of a colloid, and one analogous to the sedimentation-diffusion equilibrium obtained in an ultra centrifuge.
- d. Electrophoretic studies of soluble organic preparations such as amino acids.

7. In deriving an expression for the amount of precipitate brought down in a system of polysaccharide (S) and antibody (A), Heidelberger assumed equal specific reaction rate constants for the reactions  $AS \rightarrow ASA$  and  $AS + A \rightarrow ASAS$ . The equations for these and the reaction  $ASAS \rightarrow AS + A$  are as follows:

Actually the first constant is about twice the second constant according to reaction kinetics.

Reference:

M. Heidelberger, Chem. Rev., 24, 323 (1939)

8. While there is good evidence that antibodies are effectively bivalent in their reactions with antigens, the possibility that they are actually synthesized as monovalent molecules with an inherent tendency to dimerize with other antibody molecules or with normal globulin is worth considering. Such a hypothesis simplifies the explanation of the formation of antibodies and accounts for an observed effect of a foreign antiserum in an antigen-antibody system. Thesis, page 55. There is some evidence that normal globulins in general are equilibrium mixtures and little evidence that they are not.

9. The existence in nature of innumerable optically active substances has caused much speculation and many complicated and unreasonable theories concerning the origin of life. A simple and logical explanation of the natural optical activity is that the molecules involved directly in reproduction are optically active and can pair with or give rise to molecules only of the same kind. Even if the earliest life existed as two optical isomeric forms, it is inconceivable that both forms would have evolved into present day species of life, identical except for the optical isomerism.

10. In the interests of getting better propositions for the final examination, one of the requirements for admission to candidacy should be the submission of five propositions with brief explanations. After his experience with these preliminary propositions, the candidate would realize that developing good propositions requires much time and effort and he would have better final propositions.